

AN EXPERIMENTAL INVESTIGATION ON INDOOR RSSI-BASED LOCALIZATION

A THESIS SUBMITTED TO
THE GRADUATE SCHOOL OF NATURAL AND APPLIED SCIENCES
OF
MIDDLE EAST TECHNICAL UNIVERSITY

BY

MERİÇ KORAY KARAKURT

IN PARTIAL FULFILLMENT OF THE REQUIREMENTS
FOR
THE DEGREE OF MASTER OF SCIENCE
IN
ELECTRICAL AND ELECTRONICS ENGINEERING

AUGUST 2013

Approval of the thesis:

AN EXPERIMENTAL INVESTIGATION ON INDOOR RSSI-BASED LOCALIZATION

submitted by **MERİÇ KORAY KARAKURT** in partial fulfillment of the requirements for the degree of **Master of Science in Electrical and Electronics Engineering Department, Middle East Technical University** by,

Prof. Dr. Canan Özgen

Dean, Graduate School of **Natural and Applied Sciences**

Prof. Dr. Gönül Turhan Sayan

Head of Department, **Electrical and Electronics Engineering**

Assoc. Prof. Dr. Ali Özgür Yılmaz

Supervisor, **Electrical and Electronics Engineering Dept., METU**

Examining Committee Members:

Prof. Dr. Yalçın Tanık

Electrical and Electronics Engineering Department, METU

Assoc. Prof. Dr. Ali Özgür Yılmaz

Electrical and Electronics Engineering Department, METU

Assoc. Prof. Dr. Elif Uysal Bıyıkoğlu

Electrical and Electronics Engineering Department, METU

Assoc. Prof. Dr. Umut Orguner

Electrical and Electronics Engineering Department, METU

M.Sc. Uğur Güngör

Electronic Design Department, ASELSAN, MGEO

Date:

I hereby declare that all information in this document has been obtained and presented in accordance with academic rules and ethical conduct. I also declare that, as required by these rules and conduct, I have fully cited and referenced all material and results that are not original to this work.

Name, Last Name: MERİÇ KORAY KARAKURT

Signature :

ABSTRACT

AN EXPERIMENTAL INVESTIGATION ON INDOOR RSSI-BASED LOCALIZATION

Karakurt, Meriç Koray

M.S., Department of Electrical and Electronics Engineering

Supervisor : Assoc. Prof. Dr. Ali Özgür Yılmaz

August 2013, 66 pages

In this study, received signal strength indicator (RSSI) based indoor localization is investigated in sparse-anchor-deployment environments. Multipath propagation, dynamical variations in propagation model parameters and antenna patterns which are three of many potential error sources of indoor RSSI-based localization are experimentally analyzed. Possible enhancements so as to minimize the effects of mentioned problems are examined. A multichannel maximum-likelihood estimation (MLE) algorithm is proposed and implemented in a testbed together with some existing localization algorithms. A performance comparison of the implemented methods is provided. It is shown that the suggested method can increase the accuracy of indoor RSSI-based localization in low anchor density by using multichannel measurements and real-time propagation parameter estimation.

Keywords: Wireless Sensor Network, Localization, RSSI

ÖZ

İÇ MEKANDA ALINAN SİNYAL GÜCÜ GÖSTERGESİ TEMELLİ KONUM BULMA ÜZERİNE BİR DENEYSEL İNCELEME

KARAKURT, MERİÇ KORAY

Yüksek Lisans, Elektrik ve Elektronik Mühendisliği Bölümü

Tez Yöneticisi : Doç. Dr. Ali Özgür Yılmaz

Ağustos 2013 , 66 sayfa

Bu çalışmada, alınan sinyal gücü tabanlı iç mekan konum bulunması az sayıda çapa içeren yerleşim ortamlarında incelendi. İç mekan kablosuz ağda alınan sinyal gücü tabanlı konum bulunmasının çok sayıda potansiyel hata kaynağından üç tanesi olan çok yönlü yayılım, yayılım model parametrelerindeki dinamik değişimler ve anten paternleri deneysel olarak analiz edildi. Hata kaynaklarının etkilerini azaltmak için olası iyileştirmeler incelendi. Bir çok kanallı maksimum benzerlik kestirimi algoritması önerildi ve varolan bazı konum bulma algoritmalarıyla birlikte bir test düzeneğinde gerçekleştirildi. Önerilen ve varolan metodların performans karşılaştırılması verildi. Önerilen metodun iç mekan kablosuz ağda alınan sinyal gücü tabanlı konum bulma hassasiyetini birden çok kanallı ölçümleri ve gerçek zamanlı yayılım parametresi kestirimi kullanarak arttırılabileceği gösterildi.

Anahtar Kelimeler: Kablosuz algılayıcı ağlar, Konum bulma, RSSI

To my family and friends

ACKNOWLEDGMENTS

I would like to thank my supervisor Assoc. Prof. Dr. Ali Özgür Yılmaz for his guidance, and support. It was a honor to work with him for the last two years.

I would like to thank ASELSAN for their permissions for attending classes and for providing some technical equipments. Also, I would like to thank TÜBİTAK for their supports with TÜBİTAK-BİDEB M.s. scholarship.

Finally, I would like to thank my family and friends for their priceless support to me.

TABLE OF CONTENTS

ABSTRACT	v
ÖZ	vi
ACKNOWLEDGMENTS	viii
TABLE OF CONTENTS	ix
LIST OF TABLES	xii
LIST OF FIGURES	xiii
LIST OF ABBREVIATIONS	xvi
CHAPTERS	
1 INTRODUCTION	1
2 BACKGROUND ON WIRELESS SENSOR NETWORK LOCALIZATION	3
2.1 Taxonomy of WSN Localization	3
2.1.1 Range-free vs Range-based Localization	3
2.1.1.1 Angle of Arrival	4
2.1.1.2 Time of Arrival	4
2.1.1.3 Receive Signal Strength	5
2.1.2 Centralized vs Distributed Localization	5

2.1.3	Non-cooperative vs Cooperative Localization	5
2.1.4	Relative vs Global Localization	6
2.2	Key concepts for WSN Localization	6
2.2.1	Fading	6
2.2.1.1	Large-scale Fading	7
2.2.1.2	Small-scale Fading	7
2.2.2	Time and Frequency Diversity	7
2.2.3	Delay spread and Coherence Bandwidth	8
2.2.4	Propagation Models	8
2.2.5	Antenna Pattern	9
2.3	Basic WSN Localization Algorithms	9
2.3.1	Multilateration Algorithms	10
2.3.2	Multidimensional Scaling Algorithms	11
2.3.3	Maximum-likelihood Estimation Algorithms	12
3	IMPLEMENTED ALGORITHMS	15
3.1	Details of Existing Algorithms	15
3.1.1	Trilateration	15
3.1.2	Quadrilateration	16
3.1.3	MDS-MAP	18
3.1.4	Maximum-likelihood Estimation	19
3.2	Proposed Algorithm	20
3.2.1	Multichannel Refinement Methods	21

3.2.2	MLE of Reference Power and Path Loss Exponent	22
3.2.3	MLE of coordinates	24
3.3	Simulation Results for Implemented Algorithms	24
4	TESTBED IMPLEMENTATIONS	29
4.1	Experimental Setup	29
4.1.1	Sensor Nodes	29
4.1.2	Testbed Scenario Details	33
4.2	Experimental Results	34
4.2.1	Analyses of the Factors Affecting Localization Performance	34
4.2.1.1	Experiments about Multichannel Measurements	34
4.2.1.2	Experiments about Propagation Model Parameters	37
4.2.1.3	Experiments about Antenna Performances	39
4.2.2	Localization Experiments	40
4.2.2.1	Localization Experiment 1	41
4.2.2.2	Localization Experiment 2	45
4.2.2.3	Localization Experiment 3	48
5	CONCLUSION	53
APPENDICES		
A	CDF OF RMSE AND COORDINATE BIAS OF USED ALGORITHMS	55
REFERENCES		63

LIST OF TABLES

TABLES

Table 3.1	Average RMSE (in meters) of algorithms with 3 or 4 anchors when noise standard deviation is 2 dB	25
Table 3.2	Standard deviation of x and y coordinates' biases (in meters) of algorithms with 3 or 4 anchors when noise standard deviation is 2 dB	26
Table 3.3	Average RMSE (in meters) of algorithms with 3 or 4 anchors when noise standard deviation is 4 dB	26
Table 3.4	Standard deviation of x and y coordinates' biases (in meters) of algorithms with 3 or 4 anchors when noise standard deviation is 4 dB	27
Table 4.1	Arduino Uno board specifications	29
Table 4.2	The agent position numbers and the corresponding coordinates for experiment 1	41
Table 4.3	The agent position numbers and the corresponding coordinates for experiment 2	45

LIST OF FIGURES

FIGURES

Figure 1.1	A typical sensor node	1
Figure 2.1	A typical radiation pattern of the directive antenna	4
Figure 2.2	a) Non-cooperative and b) Cooperative localization schemes [32]	6
Figure 2.3	Path loss, shadowing and multipath effects [18]	7
Figure 3.1	A trilateration example in an ideal case	16
Figure 3.2	A trilateration example in an noisy case	17
Figure 3.3	A quadrilateration example in a noisy case	17
Figure 3.4	Flow chart of the proposed method	21
Figure 3.5	RSSI versus distance as path loss exponent changes	22
Figure 3.6	RSSI versus distance as reference power changes	23
Figure 4.1	Sensor node elements	30
Figure 4.2	Communication data flow of microcontrollers and XBee modules [15]	31
Figure 4.3	UART data frame structure of the API operation [15]	32
Figure 4.4	Supply voltage versus discharge time [19]	32
Figure 4.5	Four anchor TDMA scheme	33

Figure 4.6	Flow chart of the agent algorithm	34
Figure 4.7	Frequency hopping experiment 1	35
Figure 4.8	Frequency hopping experiment 2	36
Figure 4.9	Frequency hopping experiment 3	36
Figure 4.10	Frequency hopping experiment 4	37
Figure 4.11	RSSI deviation as battery droops in time	38
Figure 4.12	Antenna height versus RSSI measurements	39
Figure 4.13	Orientation versus RSSI measurements	40
Figure 4.14	RMSE performances of algorithms with three wire antenna anchors	42
Figure 4.15	RMSE performances of algorithms with three chip antenna anchors	42
Figure 4.16	RMSE performances of algorithms with four wire antenna anchors	43
Figure 4.17	RMSE performances of algorithms with four chip antenna anchors	44
Figure 4.18	Bias performance of MLE with different refinements methods in three anchor case	45
Figure 4.19	RMSE performances of algorithms with three 0 degree orientation chip antenna anchors	46
Figure 4.20	RMSE performances of algorithms with three 225 degrees orientation chip antenna anchors	46
Figure 4.21	RMSE performances of algorithms with four 0 degree orientation chip antenna anchors	48
Figure 4.22	RMSE performances of algorithms with four 225 degrees orientation chip antenna anchors	49
Figure 4.23	Bias performance of MLE with different refinements methods in three anchor case	49

Figure 4.24 Measured RSSI between sensor node pairs in time and RMSE of the algorithms when the agent is at (2.0,5.0)	51
Figure 4.25 Estimated P_0 and PLE values when the agent is at (2.0,5.0)	51
Figure 4.26 Measured RSSI between node pairs in time and RMSE of the algorithms when the agent is at (3.5,3.5)	52
Figure 4.27 Estimated P_0 and PLE values when the agent is at (3.5,3.5)	52
Figure A.1 CDF of Trilateration RMSE and Bias in 3 anchors with error std=2 case	56
Figure A.2 CDF of MDS RMSE and Bias in 3 anchors with error std=2 case	56
Figure A.3 CDF of MLE RMSE and Bias in 3 anchors with error std=2 case	57
Figure A.4 CDF of Quadlateration RMSE and Bias in 4 anchors with error std=2 case	57
Figure A.5 CDF of MDS RMSE and Bias in 4 anchors with error std=2 case	58
Figure A.6 CDF of MLE RMSE and Bias in 4 anchors with error std=2 case	58
Figure A.7 CDF of Trilateration RMSE and Bias in 3 anchors with error std=4 case	59
Figure A.8 CDF of MDS RMSE and Bias in 3 anchors with error std=4 case	59
Figure A.9 CDF of MLE RMSE and Bias in 3 anchors with error std=4 case	60
Figure A.10 CDF of Quadlateration RMSE and Bias in 4 anchors with error std=4 case	60
Figure A.11 CDF of MDS RMSE and Bias in 4 anchors with error std=4 case	61
Figure A.12 CDF of MLE RMSE and Bias in 4 anchors with error std=4 case	61

LIST OF ABBREVIATIONS

AoA	Angle of arrival
GPS	Global positioning system
IEEE	Institute of electrical and electronics engineers
MCU	Microcontroller unit
MDS	Multidimensional scaling
MLE	Maximum likelihood estimation
PLE	Path loss exponent
RMSE	Root mean squared error
RSSI	Received signal strength indicator
ToA	Time of arrival
TDoA	Time difference of arrival
WSN	Wireless sensor network

CHAPTER 1

INTRODUCTION

A Wireless Sensor Network (WSN) is a network composed of a number of compact devices known as sensor node. A sensor node, illustrated in Figure 1.1, usually contains a radio transceiver, microcontroller unit (MCU), memory, battery, analog to digital converter (ADC) and various sensing units. It can be used to sense various physical entities such as motion, position, humidity, temperature, radiation, etc. Sensor nodes in the same wireless sensor network communicate with each other and/or the base station in order to report sensed events. WSNs are used in many fields such as node positioning (localization), agricultural applications, health-care monitoring, asset tracking, smart structures and so on [47].

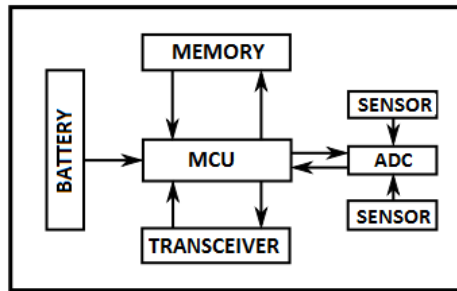


Figure 1.1: A typical sensor node

Localization can be described as the process of finding out the physical position of an object. The problem of WSN localization is to estimate the unknown coordinates of nodes (agents) in the WSN as accurately as possible. In WSN localization, different techniques are used to locate the agents. Connectivity, received signal strength, directionality of a transmitted signal, time propagation information or a combination of these are utilized by a localization algorithm to translate them to position estimates. To globally locate agents, nodes with known coordinates (anchors) are used as reference points.

The most well-known localization solution is the Global Positioning System (GPS) [28]. In this method, distances to preferably four or more GPS satellites are estimated using time difference of arrival information and the position of the GPS receiver is obtained by finding the intersections of constructed spheres. Although GPS is an innovative approach, it may not be feasible for some applications due its high cost, large size, power consumption and satellite

line-of-sight requirement. For this reason, WSN localization methods working in indoor environments and using tiny, low power and inexpensive sensor nodes have drawn considerable attention recently. As discussed in [16, 21, 31], many localization algorithms have been proposed and analyzed in different conditions so far. This study focuses on the received signal strength indicator (RSSI) based indoor localization in a sparse-anchor-deployment scenario. RSSI-based localization algorithms are investigated in depth and a number of novel algorithms utilizing different localization techniques are reviewed in the following chapter.

First goal of this study is to analyze the potential error sources of indoor RSSI-based localization experimentally and to propose some enhancements to mitigate related errors. Second goal is to implement a number of RSSI-based algorithms in different environments and to compare their performances. Most of the proposed localization methods provide successful results when many anchors are available in the localization field [21]. Nonetheless, the number of available anchors sometimes decreases sharply due to connectivity problems possibly resulting in massive performance deterioration. Thus, it is aimed to improve the performance of existing localization algorithms in sparse-anchor indoor environments. The algorithms selected for testbed implementation in this study are capable of localizing agents globally even using three anchors. Moreover, a typical sensor node has strict processor speed and memory size limitations due to its size and low power consumption requirements [16]. For this reason, instead of complex localization algorithms in the literature [21, 22, 31, 48, 52], less complicated ones are implemented in order to provide an ease of implementation and a longer battery life.

In this study, the effects of multipath fading, imperfect propagation parameter estimation and non-ideal antenna gain patterns on the RSSI measurements are investigated experimentally in the 2.4 GHz ISM band. Possible enhancements such as the usage of the multichannel measurements and real-time propagation parameter estimation are examined to minimize the effects of mentioned problems. Next, a multichannel maximum-likelihood estimation (MLE) algorithm that uses examined enhancements is proposed and implemented in a testbed together with some existing localization algorithms, namely trilateration [50], quadrilateration [13] and multidimensional scaling map (MDS-MAP) [44]. According to experimental results, it is possible to increase accuracy of the implemented algorithms. Besides, the effects of antenna types and heights of sensor nodes on the performance of the algorithms are exhibited.

The rest of this study is organized as follows:

In Chapter 2, the background information about WSN localization is given. A taxonomy and key concepts of WSN localization are mentioned and basic localization algorithms are introduced. In Chapter 3, details of the algorithms to be implemented are discussed in depth. In Chapter 4, after specifications of the testbed are stated, obtained experimental results and performance comparisons of the implemented algorithms are given. Finally, Chapter 5 summaries and concludes the study.

CHAPTER 2

BACKGROUND ON WIRELESS SENSOR NETWORK LOCALIZATION

2.1 Taxonomy of WSN Localization

A possible taxonomy of localization can be given as range-free/range-based, centralized/distributed, non-cooperative/cooperative and relative/global localization [43, 47]. Details of the categorization above are summarized as follows.

2.1.1 Range-free vs Range-based Localization

In range-free localization, only the connectivity information is used so as to determine the locations of agents. For instance, two nodes are labeled as connected when they can communicate with each other or when the measured signal strength in between is larger than a threshold, otherwise they are labeled as unconnected. Next, those binary information are utilized by connectivity based algorithms. Also, range-free localization includes fingerprinting methods [5, 23] in which the measurement characteristics of sensor nodes (fingerprints) are recorded and compared with a previously constructed database in order to estimate the position of agents. Range-free localization is cost-effective since there is no need of any extra hardware or complicated propagation modeling. This approach can be favorable in large scale localization environments with high node density. On the other hand, it may not provide accurate results in anisotropic or low node density environments due to its coarse sensing. A more detailed study on connectivity based techniques is provided in [17].

In range-based localization, the estimates of distances between sensor nodes are utilized to localize the agents. Measurement techniques in range-based WSN localization can be divided into three groups as: Angle of Arrival, Time of Arrival (or Time Difference of Arrival), Receive Signal Strength.

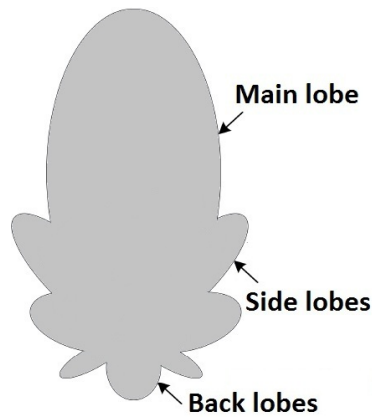


Figure 2.1: A typical radiation pattern of the directive antenna

2.1.1.1 Angle of Arrival

In angle of arrival (AoA) based methods, the directionality of transmitted signals is used in order to estimate the position of the receiver. RF transceivers, radio antenna arrays (RF propagation), ultrasound transceivers, microphone arrays (acoustic propagation), light emitters and optical sensors (light propagation) are equipments used to estimate the AoA. In AoA-based methods, receiver antenna amplitude or phase responses are often utilized. Amplitude response techniques benefit from the anisotropy in the pattern of antennas. As illustrated in Figure 2.1, a typical radiation pattern of a directional antenna has a non-uniform shape. Therefore, the direction of the agent can be estimated by finding the direction at which the maximum signal power is measured. For this purpose, an antenna array, a rotating receiver antenna or a combination of rotating and stationary receiver antennas can be used. In phase response techniques, angle of arrival information is extracted from the measurements of the phase differences in the arrival of a wave. This method requires an antenna array [30].

Generally, AoA error decreases as the number of receive antennas increases. However, accuracy of AoA measurements is limited by the pattern of the antenna, shadowing, multipath effects and non-line-of-sight conditions. Also, the requirement of additional hardware mentioned above makes AoA applications less preferable. In [4, 20, 24, 38], different approaches applying the AoA method are explained in detail.

2.1.1.2 Time of Arrival

In time of arrival (ToA) based methods, unknown distances are estimated using propagation time measurements. Sensor nodes transmit a signal (RF, ultrasound or laser wave) to their neighbors and the receiver node sends a signal back to their neighbors. The measured ToA is the time of transmission plus the propagation delay which is a function of the distance between nodes. In the Time Difference of Arrival (TDoA) techniques, the differences of arrival times of signals from a sensor node are estimated at multiple receivers and their cross-

correlations are often used to define hyperbolas between receivers on which the agent may exist. Moreover, sensor nodes may transmit two signals that travel at different speeds. For instance, radio and ultrasound transmitters are utilized together in [36]. In general, TDoA is affected less by multipath propagations than ToA [9].

Time of arrival techniques can be very accurate in line-of-sight and echo-free conditions. However, the localization performance may be poor without perfect time synchronization and delay calculation. Additionally, high cost and complexity of the structure, variations of the speed of waves with temperature and humidity and multipath vulnerability are the other disadvantages. In [8, 32, 36, 45], details on ToA and TDoA techniques can be found.

2.1.1.3 Receive Signal Strength

In receive signal strength based methods, the power measured by receiver's received signal strength indicator (RSSI) circuitry is related to the distance information via proposed propagation models. For instance, the received signal power is modeled such that it decays proportional to the square of the distance. Since most of the sensor nodes today have RSSI circuitry, measuring RSSI does not require an additional hardware. This fact increases the popularity of RSSI-based methods [33]. On the other hand, RSSI measurements suffer from shadowing and multipath fading problems similar to previously discussed methods. Additionally, the non-uniform nature of antenna patterns may affect the performance of RSSI-based methods [7, 27]. Since this study focuses on the RSSI-based localization, detailed information on RSSI-based techniques are to be provided later. Also, exhaustive information on RSSI-based methods can be found in [13, 39, 40].

2.1.2 Centralized vs Distributed Localization

In centralized localization, a central processing unit determines the location information of each unknown node in the network. First, the connectivity or range estimates between all sensor node pairs in the network are sent to the processing unit. Then, a centralized algorithm estimates the location of each sensor node in the network. In distributed localization, each sensor node itself tries to explore its location and then forward that information to other nodes in the network. Distributed techniques may be more robust and energy efficient especially for large networks. However, centralized methods can provide more accurate results since the central unit have a detailed information about the whole WSN.

2.1.3 Non-cooperative vs Cooperative Localization

In non-cooperative localization, each agent can only communicate and share information with anchors when there is an one-hop (direct link between two nodes) connection in between. Thus, an agent needs to have one-hop connection with a number of anchors in order to be

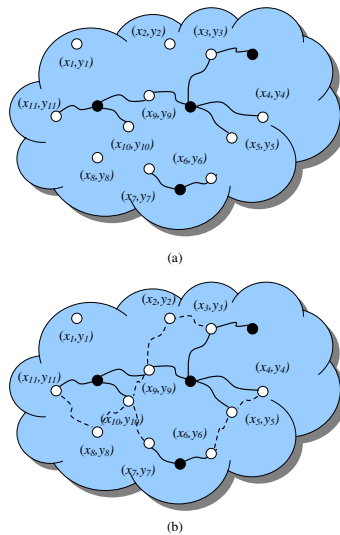


Figure 2.2: a) Non-cooperative and b) Cooperative localization schemes [32]

localized. Conversely, every sensor node in the network collaborate with each other in the cooperative approach. An agent does not need direct connections with anchors, because there is cooperative information sharing in the WSN.

Cooperative localization is more complex and complicated compared to the non-cooperative one. However, it can offer better accuracy and coverage in environments where one hop connections are rare. However, distances between nodes calculated by multi-hop connections may not be equal to euclidian distances which results in error. In Figure 2.2, where anchors and agents are demonstrated by black and white circles respectively, non-cooperative and cooperative localization schemes are illustrated. It is shown that the cooperation between the sensor nodes increases the connectivity.

2.1.4 Relative vs Global Localization

Relative localization refers to localization in a local coordinate system. There is no need of anchors for the construction of a relative map. Global localization is described as localization in a previously determined global map. Anchors are needed as reference points in order to construct a global map.

2.2 Key concepts for WSN Localization

2.2.1 Fading

The term fading can be described as the fluctuation of the amplitude of a signal in time or space [37]. It can be divided into two groups as follows.

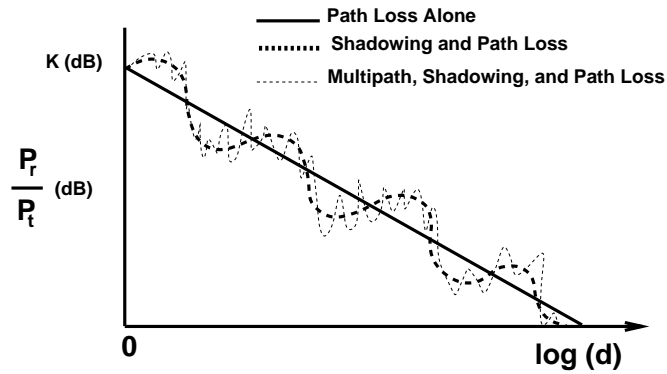


Figure 2.3: Path loss, shadowing and multipath effects [18]

2.2.1.1 Large-scale Fading

Path loss is the reduction in power of a transmitted wave as it propagates in the air. Shadowing is caused by the obstacles between the transmitter and receiver that prevent signal propagation. The obstacles between the transmitter and receiver nodes may absorb the transmit power so that the signal may be distorted. Variations due to path loss and shadowing occur over distances larger than the transmission wavelength. Therefore, those variations are referred as large-scale fading [18].

2.2.1.2 Small-scale Fading

Multipath is the phenomenon that cause radio signals to reach the receiving antenna by more than one path. Multipath signals are summed at the receiver and produce distortion in the received signal relative to the transmitted signal. Variations due to multipath usually occur over distances in the order of the transmission wavelength. Therefore, those variations can be referred as small-scale fading [18].

In Figure 2.3, the ratio of the received-to-transmit power in decibel (dB) versus log-distance for the effects of path loss, multipath and shadowing are illustrated. In fact, localization performance may be compromised or even become impossible if WSN signals fade. This issue becomes more critical in sparse anchor environments since information sources are very few.

2.2.2 Time and Frequency Diversity

Diversity methods are used to combat errors due to time or frequency dependent channel effects. Time diversity is transmitting the same data multiple times such that the likelihood of correct reception is enhanced. To be able to use time diversity, coherence time of the channel should not be very long [18]. Otherwise, retransmitting data after a time delay is pointless due

to channel measurements' still being correlated. Frequency diversity is transmitting the same data using different carrier frequencies. Channel should be frequency selective to be able to use frequency diversity.

2.2.3 Delay spread and Coherence Bandwidth

Delay spread can be described as the time between first and last multipath signals to be summed at the receiver. Coherence bandwidth may be defined as the maximum bandwidth over which frequencies of a signal experience comparable fading. Delay spread can be roughly approximated as the inverse of coherence bandwidth [18]. Using this approximation, frequency hopping across a bandwidth surpassing the reciprocal of the delay spread is adequate to obtain multiple uncorrelated measurements. To illustrate, the delay spread of indoor environments is less than 200 ns at 2.4 GHz [51]. Therefore, a five-megahertz-frequency-hopping may result in obtaining uncorrelated measurements in indoor environments.

2.2.4 Propagation Models

A propagation model characterizes the radio wave propagation as a function of environmental variables. It can be either empirical (statistical) or deterministic (theoretical), or a combination of both. While empirical models are constructed by measurements, theoretical models are based on fundamental principles of radio wave propagation [1]. The most important and frequently employed path loss models for indoor propagation scenarios are the Free Space model, One-Slope model, Multi-Wall-Floor model, and ITU indoor path loss model [12].

Due its simplicity and succeeding performance, the log-normal shadowing model which is the normal distributed version of the One-Slope model is widely used [17]. In this model, measured power is expressed as

$$\hat{p}(i, j) = P_0 - 10\alpha \log_{10}(d_{i,j}/d_0) + n = p(d_{i,j}) + n \quad (2.1)$$

where P_0 and d_0 are reference power and distance values, $d_{i,j}$ is the distance between sensor nodes i and j , α is the path loss exponent which is between 2 and 4 typically, $p(d_{i,j})$ is the received power in error-free case and n is a zero-mean and variance- σ^2 Gaussian random variable ($\sim \mathcal{N}(0, \sigma^2)$) representing the log-normal shadowing effect. The variance, σ^2 , characterizes the variability measurements between the pairs of nodes with the same separation distance at different locations. Typically, σ^2 is between 3 and 12 dB. The received power (in dBm) at sensor node i transmitted by sensor node j is a random variable with normal distribution as given in eqn. (2.2). Thus, each RSSI sample from sensor nodes i and j is the outcome of this normally distributed random variable:

$$\hat{p}_{i,j} \sim \mathcal{N}(p(d_{i,j}), \sigma^2). \quad (2.2)$$

From eqn. (2.1), the distance estimate between sensor nodes i and j , $\hat{d}_{i,j}$, is expressed as

$$\hat{d}_{i,j} = d_0 \cdot 10^{((P_0 - \hat{p}_{i,j})/10 \alpha)} = d_{i,j} \cdot 10^{(-n/10 \alpha)} \quad (2.3)$$

where n is a sample from a zero-mean and variance- σ^2 Gaussian random variable and $10^{(-n/10 \alpha)}$ term represents the multiplicative bias factor. For RSSI-based algorithms directly utilizing the distance estimations between the agent and anchors as inputs, the first step of the localization is to convert received signal power to distance via a path loss model. Since the log-normal shadowing model has been confirmed empirically to model the variation in received power accurately in indoor environments [18], the usage of eqn. (2.3) is a preferred method to transform the received power measurements to the distance estimates.

2.2.5 Antenna Pattern

Antenna performance is another vital point for indoor RSSI localization. Naturally, WSN nodes are expected to be tiny devices; therefore, wide antennas with smooth patterns are not feasible for WSN localization. It is inevitable to use small antennas with non-isotropic gain patterns. Such antennas' performance differs from device to device even for the same manufacturer as illustrated in [14]. Antenna height also affects localization results. In fact, an antenna may behave differently as the antenna height varies. In [27], it is experimentally shown that changing receiver antenna heights from three meters to half meter, the received power may decrease to one-sixteenth of its maximum value. Moreover, in [7] the effects of relative elevation and relative orientation of sensor node antennas are investigated. Various experiments are conducted in two environments in a complex indoor environment with many building components and an almost empty indoor environment. According to the results of experiments, the changes in the elevation and orientation causes variability in RSSI readings. However, due to the fact that the results are inconsistent between the two testbeds, it is concluded that the effects of these parameters on RSSI values are highly dependent on the testing environment.

2.3 Basic WSN Localization Algorithms

Recently, wireless sensor network localization has been a popular research area and investigated through many different points of view. In [2], a survey describing the concept of sensor networks and the popular localization methods is provided. In [33], cooperative localization in WSNs, which has various localization applications, is introduced and performance bounds of measurement based statistical models are presented. In [21, 22, 31], various WSN localization approaches are reviewed, and the summaries of known localization algorithms are discussed.

In this chapter, a literature review of basic WSN localization algorithms is given. RSSI-based localization algorithms are investigated in depth and a number of novel algorithms utilizing

other localization techniques are also reviewed. The algorithms are grouped according to their similarities and relations as multilateration, multidimensional scaling and maximum-likelihood estimation algorithms.

2.3.1 Multilateration Algorithms

Multilateration uses the fact that intersection of three or more circles can provide accurate position estimates. It is applied in many algorithms either as the primary or the secondary technique.

In [50], trilateration is described in detail. The trilateration algorithm can be defined as the process of finding out the coordinates of an agent using the geometry of three circles. The circles are located at the center of anchor coordinates and their radii are determined by using the measurements between the agent and anchors. Afterwards, the agent is localized by determining the position of the intersection of the circles. Satisfactory results can be obtained by trilateration as long as the radius estimates have small errors and all the anchors do not lie on a single line.

In [28], the Global Positioning System (GPS) is described. This algorithm uses TDoA information and multilateration for localization. A GPS receiver estimates distances to at least four GPS satellites via TDoA results and then it calculates its position in 3-dimensions by finding the intersections of consisted spheres. The accuracy of this method can be between 1 and 10 meters, however it works only in outdoor environments. The one hop multilateration operation performed by GPS is extended to operate on multiple hops in [42]. This enabled agents that cannot directly communicate with anchors to collaborate with non-anchor nodes.

In [29], a distributed localization algorithm, called the Ad Hoc Positioning System (APS), is proposed. In APS, the capabilities of anchors are extended to non-anchor nodes by a hop by hop method. It is based on a hybrid method combining the distance vector propagation and the GPS localization. The distance vectors can be represented using hop counts (DV-Hop), RSSI-based estimated distances (DV-Distance), or Euclidean distances. According to simulation results, APS can be one-hop accurate. In [30], APS using the angle of arrival technique is proposed. In this method, agents' position and orientation are estimated in a network where nodes can measure angle of arrival (AoA) from their neighbors. It is shown via simulations that proposed algorithm is as accurate as ranging based APS, and orientation estimates are beneficial for tracking applications.

An iterative multilateration algorithm that uses multilateration is proposed in [41]. In this algorithm, ultrasound-based TDoA measurements are utilized iteratively with a distributed way. According to simulation results, the ultrasound-based TDoA technique is less sensitive to physical effects than RSSI-based methods.

In [13], an improved quadrilateral localization algorithm is introduced. In this algorithm, a flip ambiguity detection criterion is added to the trilateration method to attain more accurate lo-

calization results. Then, centroid quadrilateral localization (CQL) and comparative weighted quadrilateral localization (WQL) algorithms are proposed by adding the fourth anchor to the localization scheme. It is experimentally shown that both WQL and CQL algorithms perform well in noisy environments.

2.3.2 Multidimensional Scaling Algorithms

In [44], a centralized WSN localization algorithm that uses metric multidimensional scaling, named MDS-MAP, is proposed. In MDS-MAP, path distances between all pairs of nodes are computed to construct a distance matrix, and multidimensional scaling (MDS) is applied to the distance matrix to derive node locations that fit the estimated distances. Then, the first 2 or 3 largest eigenvalues and eigenvectors are used to construct a 2-D or a 3-D relative map, and the relative map is transformed to a global map based on the positions of anchors. The strength of MDS is that it can work well when there are few anchors in the localization environment.

Proximity Distance Map (PDM) is proposed in [26]. PDM uses the singular value decomposition (SVD) technique to analyze the relationship between the geographic distances and the proximities similar to MDS-based methods. In PDM, SVD is applied only to the proximity matrix between anchors to decrease the complexity. The method of collecting distance and proximity information between nodes is similar to that of APS, and a linearized model based method is used as the lateration algorithm. According to simulation results given, PDM can outperform APS and MDS-MAP especially when the WSN is irregular and has adequate number of uniformly distributed anchors.

An algorithm combining two different localization techniques, MDS-MAP and PDM, is presented and named MDS+PDM in [11]. The proposed algorithm has less complexity than MDS-MAP because it utilizes the secondary anchors' information and PDM in the second phase of localization. MDS+PDM is analyzed in localization environments in which the number of anchor is low (3-10) and the number of nodes is high (50-200). By simulations, it is demonstrated that the proposed algorithm provides results as accurate as MDS-MAP and is less susceptible to anchor placement than both MDS-MAP and PDM in the described localization environments.

In [10], a weighted multidimensional scaling algorithm is proposed. To increase the localization accuracy, an iterative weighting method, namely iterative quadratic maximum-likelihood (IQML) is applied. It is shown that the estimation performance of the proposed algorithm can approach Cramer-Rao lower bound (CRLB) for small noise conditions. In [46], Improved MDS (IMDS) is proposed. In this algorithm, local positioning areas (LPA) are constructed by an adaptive search algorithm to change the centralized approach in MDS-MAP to the distributed one. Then, the shortest path distances between nodes on LPA are processed with the geometric correction method (GCM) and adjusting weight correction method (AWCM). Finally, the relative to global map translation is done via the classical MDS. IMDS is shown to be energy efficient, and to have better performance than the MDS-MAP especially when

the network topology is irregular.

2.3.3 Maximum-likelihood Estimation Algorithms

In [35], a maximum-likelihood estimation (MLE) method is proposed to calculate device coordinates using pair-wise RSSI measurements and anchor coordinates. It is the first time, an MLE method is used for wireless sensor localization problem. In this algorithm, a conjugate gradient method is applied to find the minimum of the cost function giving the ML estimates of the unknown node coordinates. It is demonstrated using RSSI measurements that sensor nodes in an indoor environment are located with a median error of 1.8 meters. By the same authors, the accuracy of single-hop range-based localization algorithms is discussed in [34]. CRBs and ML estimators under Gaussian and log-normal models for the ToA and RSSI measurements are derived. Then, it is experimentally shown that root mean squared location errors can be as good as 1 meter and 2 meters respectively for ToA and RSSI cases under the specified testbed conditions.

An integrated MDS and MLE algorithm, named MDS-MLE, is provided in [52] to benefit from the advantages of both methods. In the proposed algorithm, MDS is implemented to generate the initial values for MLE, and the unknown nodes coordinates are calculated by using MDS and MLE iteratively. According to various simulation results, performance of the MDS-MLE is better than MDS and MLE for the RSSI-based collaborative localization problem. Collaborative schemes are tested when the number of nodes are between 30-100 and the number of anchors are 4-28. In [48], an MLE-MLE algorithm is proposed based on the idea that cooperative MDS-MLE algorithm in [52] can be improved. In MLE-MLE, a non-cooperative MLE is applied to generate the initial values for the iterative MLE cooperative localization algorithm. The authors claim that the unimodal property of the single node log-likelihood guarantees that this MLE method converges to the unique solution. According to analysis conducted in different sizes of networks, MLE-MLE can achieve near CRB performance and perform better than MDS-MLE.

In [40], the joint ML estimation of the RSSI-based location and path loss exponent (PLE) is introduced. In this work, the joint conditional probability density function of observed path loss is derived by assuming the noise components from each anchors' measurements are independent and Gaussian distributed. Next, a less complex version of a previously proposed RSS-PLE joint estimator [25] is given so as to estimate the unknown coordinates and PLE iteratively. It is shown that localization performance is dramatically degraded when PLE is incorrectly assumed. Moreover, it pointed out that the ML estimate solution is equivalent to the nonlinear least square (NLS) solution.

An alternating gain and position estimation (AGAPE) algorithm is proposed in [53] to jointly estimate the orientation and the position of an agent using RSS measurements from the anchor nodes. This algorithm uses MLE to estimate the position of the agent, and the first-order sinusoidal model to estimate the orientation. As the orientation estimate changes, the position

of the agent is estimated again. This iteration is repeated until a misfit function is minimized. It is demonstrated that the accuracy of position estimates can be improved by including orientation estimates in the localization algorithm.

CHAPTER 3

IMPLEMENTED ALGORITHMS

In this chapter, details on the existing algorithms to be implemented are explained. The proposed method, a multichannel MLE algorithm, is described. Later, implemented algorithms are simulated in various environments and comparisons are made.

3.1 Details of Existing Algorithms

3.1.1 Trilateration

The trilateration [50] is the process of finding out the coordinates of an agent using the geometry of three circles as mentioned in Chapter 2. In RSSI-based trilateration, distances between the agent and anchors are usually estimated using the log-normal shadowing model described previously. In parallel to that, the diameters of trilateration circles are calculated using eqn. (2.3) in this study. A trilateration scheme, in which three anchors A, B, and C are used to locate the agent D, is illustrated in Figure 3.1. When the sensor node coordinates are denoted as (x_a, y_a) , (x_b, y_b) , (x_c, y_c) , (x_d, y_d) and the distances between each anchor and agent are shown as r_a, r_b, r_c , the following system of an equations is formed:

$$(x_a - x_d)^2 + (y_a - y_d)^2 = r_a^2, \quad (3.1)$$

$$(x_b - x_d)^2 + (y_b - y_d)^2 = r_b^2, \quad (3.2)$$

$$(x_c - x_d)^2 + (y_c - y_d)^2 = r_c^2. \quad (3.3)$$

Subtracting eqn. (3.1) from eqn. (3.2) and eqn. (3.2) from eqn. (3.3), following equations are found:

$$\begin{aligned} (x_a - x_d)^2 + (y_a - y_d)^2 - (x_b - x_d)^2 - (y_b - y_d)^2 &= r_a^2 - r_b^2, \\ (x_b - x_d)^2 + (y_b - y_d)^2 - (x_c - x_d)^2 - (y_c - y_d)^2 &= r_b^2 - r_c^2. \end{aligned} \quad (3.4)$$

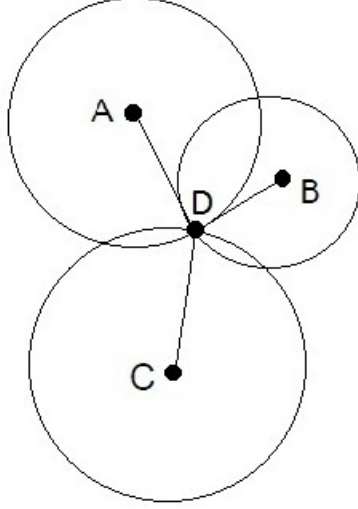


Figure 3.1: A trilateration example in an ideal case

To calculate the coordinates of the agent D directly, the matrix representation of eqn. (3.4) is written as

$$K = L^{-1}M \quad (3.5)$$

where

$$K = \begin{bmatrix} x_d \\ y_d \end{bmatrix} \quad (3.6)$$

$$L = \begin{bmatrix} 2(x_b - x_a) & 2(y_b - y_a) \\ 2(x_c - x_b) & 2(y_c - y_b) \end{bmatrix} \quad (3.7)$$

$$M = \begin{bmatrix} x_b^2 - x_a^2 + y_b^2 - y_a^2 + r_a^2 - r_b^2 \\ x_c^2 - x_b^2 + y_c^2 - y_b^2 + r_b^2 - r_c^2 \end{bmatrix} \quad (3.8)$$

Finally, eqn. (3.5) is used in order to estimate the unknown agent coordinates. This method can localize the agent accurately when the measurements are error-free, however the measurement errors are usually inevitable. As exemplified in Figure 3.2, the intersection of anchor circles is an area instead of a point when the measurements are noisy. In that case, the solution of eqn. (3.5) does not satisfy equations (3.1), (3.2) and (3.3) directly. Instead, the solution provides the coordinates such that eqn. (3.4) is satisfied.

3.1.2 Quadlateration

In the quadlateration [13], four anchors are used to locate an agent. In this method, the trilateration is applied four times and the results are averaged to obtain a better estimate. Assuming that four agent positions estimated by the trilateration are (x_{d1}, y_{d1}) , (x_{d2}, y_{d2}) , (x_{d3}, y_{d3}) , (x_{d4}, y_{d4}) , the quadlateration result is

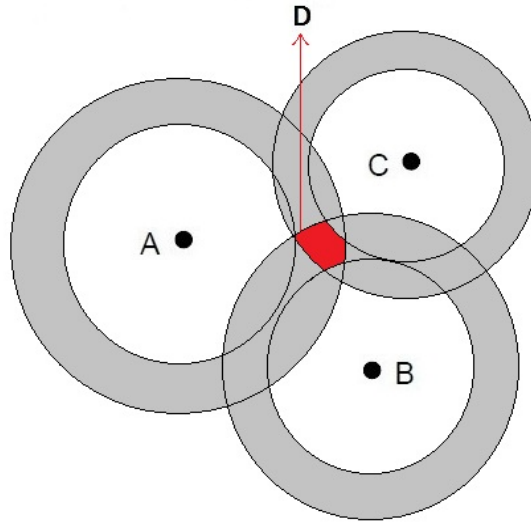


Figure 3.2: A trilateration example in a noisy case

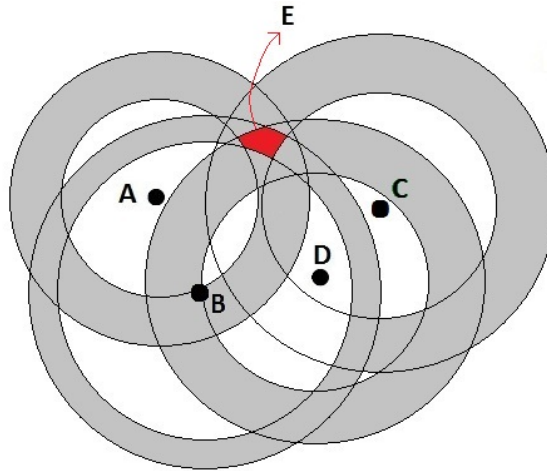


Figure 3.3: A quadrilateration example in a noisy case

$$S = \left[\frac{(x_{d1} + x_{d2} + x_{d3} + x_{d4})}{4} \quad \frac{(y_{d1} + y_{d2} + y_{d3} + y_{d4})}{4} \right] \quad (3.9)$$

Quadrilateration tends to provide more accurate results compared to trilateration at the expense of using one more anchor. On the other hand, localization performance may be deteriorated when the measurements between the agent and fourth anchor contains huge errors. Also, in some indoor localization environments the agent may not have communication with four anchors so that the quadrilateration implementation is not possible. A quadrilateration example in a noisy case is provided in Figure 3.3.

3.1.3 MDS-MAP

As mentioned in Chapter 2, MDS-MAP [44] is a localization algorithm based on multidimensional scaling. It utilizes an input matrix containing distances between pairs of nodes and find out a coordinate matrix whose configuration minimizes a loss function. One may refer to [6] for a more detailed explanation. Provided that the positions of a sufficient number of anchors are known, e.g., 3 anchors for 2-D localization, MDS-MAP determines the absolute coordinates of nodes in the network. The method is to minimize the sum of squares of the errors between the true positions of the anchors and their transformed coordinates. Similar to RSSI-based trilateration, the distances between sensor nodes are estimated using eqn. (2.3) in this study. The overall algorithm can be explained in three main steps as follows:

1) Estimate the path distances between all pairs of nodes to construct the distance matrix D ;

$$D = \begin{bmatrix} d_{11} & \cdots & d_{1j} \\ \vdots & \ddots & \vdots \\ d_{i1} & \cdots & d_{ij} \end{bmatrix} \quad (3.10)$$

where d_{ij} is the distance between i th and j th nodes. Since d_{ij} is zero when $i=j$, the diagonal of D is zero. Also, D is a symmetric matrix since $d_{ij}=d_{ji}$ for all i and j . The pairwise distances between agents and anchors are the only unknown terms in D since the distances between anchors are known by the system. To illustrate, when there is 1 agent and 3 anchors in the localization area, D becomes

$$D = \begin{bmatrix} 0 & d_{12} & d_{13} & d_{14} \\ d_{12} & 0 & d_{23} & d_{24} \\ d_{13} & d_{23} & 0 & d_{34} \\ d_{14} & d_{24} & d_{34} & 0 \end{bmatrix} \quad (3.11)$$

where d_{12} , d_{13} , d_{14} are the distances between agent-anchor pairs and d_{23} , d_{24} , d_{34} are the known distances between anchors. The algorithm can locate the agent provided that the estimates of 3 agent-anchor distances, d_{12} , d_{13} and d_{14} , are available. As mentioned before, these terms are estimated using eqn. (2.3) in this study. This approach is extended to the cases where localization environments contain more agents and/or anchors. It is important that D should not contain any unknown terms.

2) Apply classical MDS [6] to D , retain the first 2 (or 3) largest eigenvalues and eigenvectors to construct a 2-D (or 3-D) relative map. Applying classical MDS can be summarized in three sub-steps [49].

- Convert D into a double-centered matrix B ;

$$B = -\frac{1}{2} \left(I - \frac{1}{n} U \right) D^2 \left(I - \frac{1}{n} U \right) \quad (3.12)$$

where n is the number of sensor nodes used, I is a $n \times n$ identity matrix and U is a $n \times n$ matrix with all ones.

- Take the Singular Value Decomposition of B ;

$$B = VAV^T \quad (3.13)$$

- Compute the relative node coordinates matrix X ;

$$\begin{aligned} X &= VA^{1/2} \\ &= \begin{bmatrix} x_{11} & \cdots & x_{1k} \\ \vdots & \ddots & \vdots \\ x_{m1} & \cdots & x_{mk} \end{bmatrix} \end{aligned} \quad (3.14)$$

where m is equal to the number of nodes plus one and k is equal to the number of anchors minus one.

The relative x and y coordinates of the agent is written as

$$Y = \begin{bmatrix} x_{m,1} & x_{m,2} \end{bmatrix} \quad (3.15)$$

3) The coordinates of the nodes in the relative map are mapped to their absolute coordinates. This transformation is done using scaling, rotation and reflection components which are calculated using by comparing relative map coordinates and the known coordinates of the anchors. Later, transformation components are applied to the relative coordinates as follows

$$S = b * Y * T + c; \quad (3.16)$$

where c is translation component, T is orthogonal rotation and reflection component, b is scale component and S is the global coordinates of the agent.

3.1.4 Maximum-likelihood Estimation

As discussed in Chapter 2, RSSI measurements can be modeled as in eqn. (2.1). Thus, each noise sample for a measurement between sensor node pair i , n_i , is a Gaussian random variable with variance σ^2 and mean $p_i(x, y) = P_0 - 10\alpha \log_{10}(d/d_0)$ where P_0 , α , d_0 and d are reference power, path loss exponent, reference distance and distance between nodes respectively.

In a localization environment, three different observations collected at an agent can be written

as

$$\begin{aligned}
z_1 &= p_1(x, y) + n_1, \\
z_2 &= p_2(x, y) + n_2, \\
z_3 &= p_3(x, y) + n_3
\end{aligned} \tag{3.17}$$

where $p_i(x, y)$ is the reference power plus the propagation loss between the i -th anchor and the agent when the agent is located at its actual position, (x, y) .

Assuming that measurement noise samples are independent Gaussian random variables with variance σ^2 and mean $p_i(x, y) = P_0 - 10\alpha \log_{10}(d/d_0)$, the ML estimate of the agent position is expressed as

$$\begin{aligned}
(\hat{x}, \hat{y})_{MLE} &= \arg \max_{(x, y)} f(z_1, z_2, z_3 | (x, y)) \\
&= \arg \max_{(x, y)} f(z_1 | (x, y)) f(z_2 | (x, y)) f(z_3 | (x, y)) \\
&= \arg \max_{(x, y)} \left(\frac{1}{(2\pi\sigma^2)^{1/2}} \right) \exp \left(\frac{-\sum_{i=1}^N (z_i - p_i(x, y))^2}{2\sigma^2} \right) \\
&= \arg \min_{(x, y)} \sum_{i=1}^N (z_i - p_i(x, y))^2
\end{aligned} \tag{3.18}$$

Unlike multilateration methods and MDS-MAP that directly utilize the distance between sensor nodes estimated via the log-normal shadowing model, RSSI-based joint maximum-likelihood estimation method tries to minimize the sum of squares of the measurement errors of all anchor-agent pairs. In other words, instead of assuming the anchor-agent distances are known, this method tries to find out the most suitable agent position that is compatible with all RSSI measurements.

Additionally, when the path loss model parameters are also used to estimate the agent location instead of assuming that they are constant, eqn. (3.18) becomes

$$(\hat{x}, \hat{y})_{MLE} = \arg \min_{(\phi)} \sum_{i=1}^N (z_i - p_i(x, y))^2 \tag{3.19}$$

where $\phi = [x, y, \alpha, P_0]$ includes the unknown coordinates, the path loss exponent, the reference power and N is the number of anchors. In this approach, the solution is much more complex but it may provide more accurate localization results.

3.2 Proposed Algorithm

To estimate the coordinates of the agents, a three stage multichannel MLE algorithm whose flow chart is given in Figure 3.4 is proposed. In the first stage, the algorithm refines the collected multichannel RSSI measurements. In the second stage, it estimates the path loss

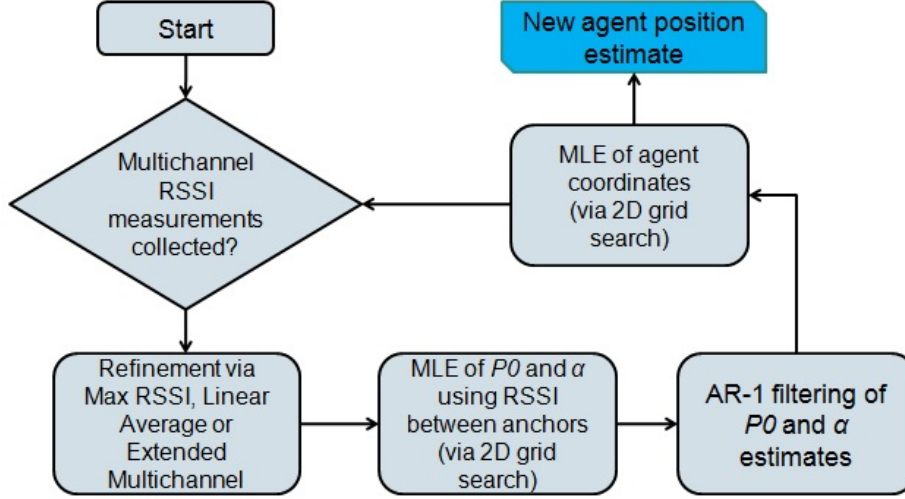


Figure 3.4: Flow chart of the proposed method

exponent and the reference power using RSSI measurements between the anchors and filters out the high-frequency components of measurements. Lastly, the algorithm conducts ML estimation of the agent coordinates using refined RSSI measurements and estimated model parameters.

3.2.1 Multichannel Refinement Methods

As mentioned in Section 2.2, frequency diversity is an important technique to combat multipath propagation. Although the effect of usage of multichannels on RSSI measurements are analyzed experimentally previously, either its effects on different range-based RSSI algorithms are not investigated or obtained results are abstracted from localization algorithms. In addition, the average of the multichannel measurements are often utilized even though alternative approaches are possible. In [5], the averages of multichannel measurements in the 2.4 GHz ISM band are used with two different range-free fingerprinting algorithms and shown that localization accuracy can be improved. However, a proximity algorithm, that uses signal strength as a direct distance metric, is shown to perform worse with the usage of multichannel measurements. Also, in [3] it is reported that IEEE 802.15.4 multichannel transmissions in the 2.4 GHz ISM band can improve RSSI-based measurements.

In the light of these, three different refinement methods are added to the proposed method to smooth the effects of multipath propagation. These methods are explained below. Performance comparisons of them are to be provided later.

• **Linear Scale Average:** In this method RSSI samples are averaged over frequency. Multichannel measurements are converted to milliwatt (mW) from dBm and averaged as follows

$$Pr = 10 \log_{10} \sum_{j=1}^k \left(\frac{(10^{(Pr_j/10)})}{k} \right) \quad (3.20)$$

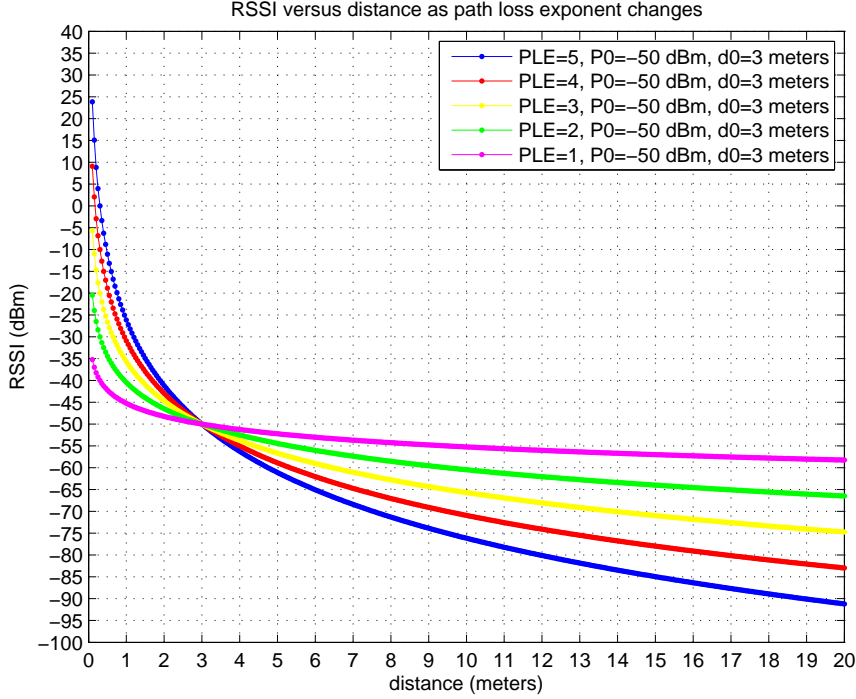


Figure 3.5: RSSI versus distance as path loss exponent changes

where k is the number of frequency hops.

- **Maximum RSSI:** This method selects the maximum RSSI value among multiple channel measurements with the idea that low power readings are not reliable. Formulation is

$$Pr = \max_{i \in 1 \dots k} (Pr_i) \quad (3.21)$$

where k is the number of frequency hops.

- **Extended Multichannel:** In this method, the algorithm uses multichannel measurements as independent observations. In other words, estimation calculations are done as if the number of anchors times the number of communication channel measurements exists. For instance, when there are three anchors in the localization field and three different channels are available, the algorithm uses nine (3×3) RSSI measurements for each localization estimation.

3.2.2 MLE of Reference Power and Path Loss Exponent

The log-normal model parameters, reference power and path loss exponent, may depend on the environmental conditions and change in time due to various dynamic factors such as temperature, humidity, changes in the geometry of localization environment or human traffic in the localization area etc. In Figure 3.5, RSSI measurements drawn against distance for path loss exponents varying from 1 to 5 are shown. For instance, provided that RSSI measured between a sensor pair is -60 dBm, the corresponding distance in the log-normal model is 4,75

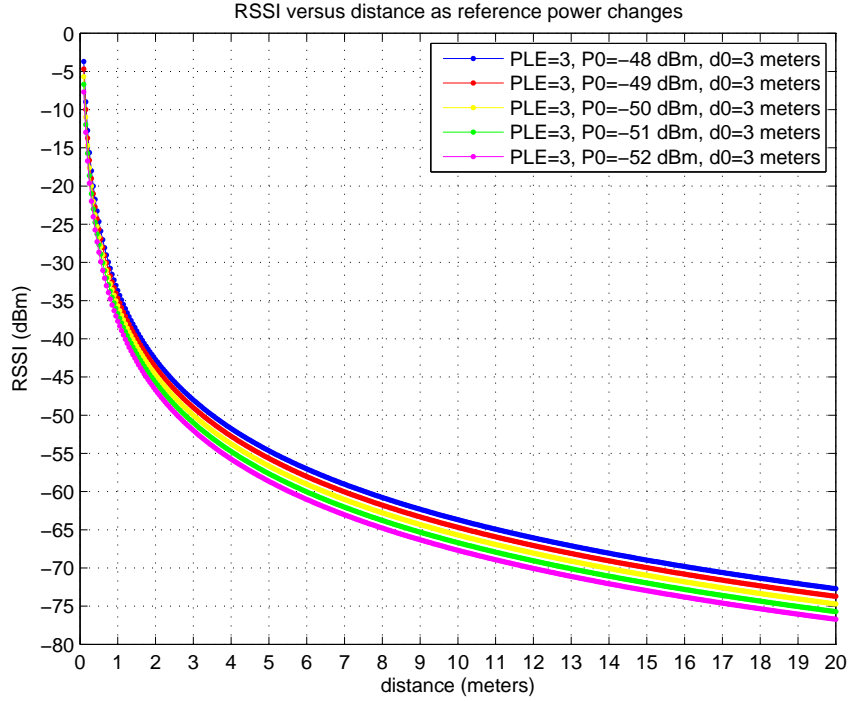


Figure 3.6: RSSI versus distance as reference power changes

meters with a PLE of 5. On the other hand, when PLE is 3 the corresponding distance to the same RSSI value is around 6,70 meters. In Figure 3.6, RSSI measurements drawn against distance for the reference powers from -52 dBm to -48 dBm are shown. To illustrate, provided that RSSI measured between a sensor pair is -60 dBm, the corresponding distance in the log-normal model is 4,75 meters with a reference power of -48 dBm. On the other hand, when the reference power is -52 dBm the distance corresponding to the same RSSI value is around 7,65 meters. Therefore, the distances between sensor node pairs are interpreted wrong when the actual model parameters are not used. The assumption that the log-normal model parameters is constant for any localization environment may significantly decrease the accuracy of the localization algorithms.

To prevent such errors, the proposed algorithm estimates PLE and P_0 using recent RSSI measurements between anchors. As the distances between the anchors are known, only PLE and P_0 are unknown in eqn. (3.19). The algorithm performs a 2-D grid search and estimates both parameters. Step sizes of PLE and P_0 are selected judiciously as 0.1 and 0.5 dBm. According to the Monte Carlo simulations carried out in MATLAB, smaller step sizes are not increasing the accuracy of estimates significantly while they are increasing the computational complexity. Next, PLE and P_0 estimates are separately provided to an autoregressive filter of order 1 (AR-1). The purpose of this operation is to smooth the estimation noise. The mentioned AR-1 filter is written as follows

$$y[n] = a * y[n - 1] + b * x[n] \quad (3.22)$$

where $x[n]$ is the ML estimate of PLE or P_0 at time n , $y[n-1]$ is the output of the filter at time $n-1$, a and b the filter coefficients. The values of a and b are judiciously selected as 0.8 and 0.2 according to simulations on MATLAB.

3.2.3 MLE of coordinates

In this stage, another 2-D grid search is performed to minimize eqn. (3.19) using the PLE and P_0 values estimated previously. The proposed method first finds the minimum of cost function using coarse step sizes for x and y coordinates and determines the grid point where the agent is possibly located. Afterwards, it scans the selected grid with more precise step sizes to estimate the position of the agent. Coarse and precise step sizes for x and y coordinates are judiciously set to 10 percent and 2 percent of maximum values of x and y coordinates. For instance, if the localization area is a 10 m by 10 m room, initial step sizes for x and y coordinates are both 1 m and secondary step sizes are both 0.2 m. This approach reduces calculation cycles without decreasing the localization accuracy significantly according to the Monte Carlo simulations conducted in MATLAB. On the other hand, one may directly apply 2-D grid search with 0.2 meter step sizes but its computational complexity would be much larger. Minimization to find the agent coordinates can also be done via numerical search methods like steepest descent or Gauss-Newton methods. Nonetheless, those methods may have high computational complexity and require good initialization points in order not to converge to local minima. In today's technology 2-D grid search can be accomplished quickly and successfully even by the cheapest microcontrollers. For these reasons, the proposed algorithm utilizes two distinct 2-D grid searches, the first one is for reference power and path loss exponent and the second one is for x and y coordinates of the agent. Eventually, the agent location is estimated. The grid search boundaries are generic inputs to the algorithm. They can be set specifically for a localization environment or fixed to typical limits (for instance, between 2 and 5 for PLE) to decrease the computational load. Instead of two consecutive 2-D grid searches, a direct 4-D grid search could also be conducted as shown in eqn. 3.19, however its high computation cost prevent its usage in real-time applications [53].

3.3 Simulation Results for Implemented Algorithms

In this section, implemented algorithms are simulated under various conditions to have an idea about algorithms' performances before the testbed applications. The effects of noisy RSSI measurements and number of anchors on the localization accuracy of the implement algorithms are analyzed. Since this study focuses on WSN localization in low anchor density, three or four anchors are placed at the corners of a 10 m by 10 m simulation area. The agent is located at various positions with 0.5 meter increments in x or y directions. Thus, an agent position can expressed as

Table3.1: Average RMSE (in meters) of algorithms with 3 or 4 anchors when noise standard deviation is 2 dB

Algorithm	Ch 1 only	Ch 2 only	Max RSSI	Linear Avg	Ext-MCH
MLE-3	1.28	1.29	1.18	0.97	0.95
MDS-3	1.71	1.72	1.52	1.27	-
TRLT-3	1.97	1.98	1.66	1.48	-
MLE-4	1.04	1.03	0.84	0.77	0.76
MDS-4	1.54	1.52	1.32	1.12	-
QUAD-4	1.56	1.54	1.30	1.13	-

$$a_i = \left(\frac{k+1}{2}, \frac{m+1}{2} \right), \quad 0 \leq k \leq 18, \quad 0 \leq m \leq 18 \quad (3.23)$$

where $1 \leq i \leq 361$.

The actual RSSI values for each deployment are calculated by using known distances between the sensor pairs and summed with normally distributed random variables with a mean value of 0 and a standard deviation of either 2 or 4 dB. To observe the effects of refinement methods, two independent RSSI values are calculated for each deployment as if there are multiple communication channels between sensor nodes. For each agent position, one hundred Monte Carlo simulations are carried out and then root mean squared error (RMSE) and bias of each algorithm is calculated. Finally, the average of RMSE and variance of the x and y coordinates' biases of the algorithms are calculated using the results of 361 cases to compare the overall error performances of implemented algorithms. Additionally, empirical cumulative distribution functions (CDFs) of the RMSE and bias of each algorithm under specified conditions are provided in Appendix A. Comments on RMSE and variance of bias performances of the implemented algorithms are in order. MLE, MDS and multilateration (trilateration and quadrilateration) algorithms that uses 3 and 4 anchors are abbreviated as MLE-3, MDS-3, TRLT-3, MLE-4, MDS-4 and QUAD-4, all respectively.

In the first set of simulations, the measurement noise samples are independent Gaussian random variables with a mean of 0 and a standard deviation of either 2 dB. Performances of the algorithms using 3 or 4 anchors are given in Tables 3.1 and 3.2. The major outcomes of simulation results are summarized as follows:

- An important observation from Table 3.1 is that all algorithms using 3 anchors and refinement methods can either outperform or perform as well as themselves using 4 anchors and no refinements. For instance, average RMSE of MLE-3 with linear average and extended multichannel is slightly better than MLE-4 without refinements. Also, RMSE of MDS-3 and TRLT-3 with refinements are very close to RMSE of MDS-4 and QUAD-4 without refinements. Since the number of anchors an agent has communication is limited in indoor localization environments, it is valuable to observe that algorithms using refinements methods can provide similar RMSE performances when they use fewer anchors.

Table3.2: Standard deviation of x and y coordinates' biases (in meters) of algorithms with 3 or 4 anchors when noise standard deviation is 2 dB

Algorithm	Ch 1 only	Ch 2 only	Max RSSI	Linear Avg	Ext-MCH
MLE-3	(0.22,0.22)	(0.22,0.22)	(0.38,0.38)	(0.17,0.17)	(0.16,0.14)
MDS-3	(0.30,0.30)	(0.30,0.30)	(0.59,0.60)	(0.24,0.24)	-
TRLT-3	(0.36, 0.34)	(0.36,0.36)	(0.51,0.52)	(0.28,0.26)	-
MLE-4	(0.17,0.17)	(0.17,0.17)	(0.26,0.28)	(0.14,0.14)	(0.14,0.13)
MDS-4	(0.20,0.22)	(0.20,0.22)	(0.51,0.53)	(0.17,0.20)	-
QUAD-4	(0.22,0.22)	(0.22,0.22)	(0.45,0.46)	(0.17,0.20)	-

Table3.3: Average RMSE (in meters) of algorithms with 3 or 4 anchors when noise standard deviation is 4 dB

Algorithm	Ch 1 only	Ch 2 only	Max RSSI	Linear Avg	Ext-MCH
MLE-3	2.29	2.31	2.03	1.80	1.73
MDS-3	3.09	3.12	2.54	2.38	-
TRLT-3	3.36	3.38	2.75	2.65	-
MLE-4	2.06	1.87	1.47	1.41	1.39
MDS-4	2.91	2.93	2.28	2.15	-
QUAD-4	2.90	2.91	2.27	2.16	-

- Multichannel refinements are capable of increasing the localization accuracy by at least 10 % and at most 28 % according to the results shown in Table 3.1. Additionally, MLE outperforms the other two algorithms in all conditions and the most accurate result is obtained by MLE-4 with extended multichannel refinement.

- As shown in Table 3.2, standard deviation of the bias of agent coordinates estimated by the algorithms are between 0.13 and 0.59. Addition of the fourth anchor improves bias performance of MDS and multilateration algorithms more significantly, while same improvement is less for the MLE algorithms. Also, worst bias performance is obtained with the usage of maximum RSSI refinement in both 3 and 4 anchor cases.

In the second set of simulations, the measurement noise samples are independent Gaussian random variables with mean=0 and standard deviation=4 dB. Performances of the algorithms using 3 or 4 anchors are given in Tables 3.3 and 3.4. The main results observed and their comparisons with the ones from the first set of simulations are summarized as follows:

- Comments made about average RMSEs of the algorithms in the previous set of simulations are valid in this set of simulations with the addition that RMSEs of algorithms increased in all cases due to the increase in noise power. When Tables 3.1 and 3.3 are compared, RMSEs in Table 3.3 are at least 65 % and at most 90 % higher than RMSEs in Table 3.1. Moreover, an algorithm-refinement method pair more immune to the increase in noise power is not observed.

Table3.4: Standard deviation of x and y coordinates' biases (in meters) of algorithms with 3 or 4 anchors when noise standard deviation is 4 dB

Algorithm	Ch 1 only	Ch 2 only	Max RSSI	Linear Avg	Ext-MCH
MLE-3	(0.46,0.45)	(0.46,0.46)	(0.70,0.71)	(0.44,0.43)	(0.33,0.32)
MDS-3	(0.69,0.68)	(0.70,0.73)	(1.06,1.07)	(0.64,0.65)	-
TRLT-3	(0.75,0.75)	(0.77,0.79)	(0.94,0.96)	(0.64,0.67)	-
MLE-4	(0.36,0.36)	(0.36,0.36)	(0.41,0.41)	(0.31,0.31)	(0.26,0.26)
MDS-4	(0.46,0.45)	(0.47,0.48)	(0.88,0.89)	(0.45,0.46)	-
QUAD-4	(0.46,0.46)	(0.47,0.48)	(0.79,0.80)	(0.34,0.45)	-

- Similar to the previous set of simulations, x and y coordinates have smaller bias deviations when 4 anchors are used. Therefore, it can be concluded that with the addition of the fourth anchor to the localization area the placement of anchors becomes symmetrical so that bias deviations of the location estimates of algorithms decrease independent of the usage of refinement methods. However, x and y coordinates with less bias deviations does not mean higher localization accuracy. For instance, MLE-3 with maximum RSSI has a bias deviation of (0.70,0.71) and an average RMSE of 2.03 meters while MLE-3 with single channels has a bias deviation of (0.46,0.46) and an average RMSE of 2.30 meters as observed from 3.3 and 3.4.

- A conclusion drawn from two sets of experiments is that multichannel refinements improves both average RMSE and bias deviations of the algorithms. Moreover, extended multichannel refinement provides the best RMSE and bias results among all algorithm-anchor combinations. It is an advantage over those two methods and may be significant for real world implementations.

CHAPTER 4

TESTBED IMPLEMENTATIONS

4.1 Experimental Setup

4.1.1 Sensor Nodes

Arduino Uno boards are used as wireless sensor nodes in testbed implementations. In Table 4.1, Arduino Uno board specifications are provided. ATmega328 microcontrollers are the control units of the sensor nodes. To enable wireless communication between sensor nodes, each board is extended using Arduino Wireless Shield equipped with an XBee 802.15.4 RF module. The transmit power and the receiver sensitivity of a module are, respectively, 0 dBm and -92 dBm. XBee modules with two types of antennas, namely wire and chip, are used in the experiments. Also, NiMH rechargeable 9V 200 mAh batteries are utilized as the power supplies. Sensor node elements are shown in Figure 4.1.

Table4.1: Arduino Uno board specifications

Microcontroller	ATmega328
Operating Voltage	5V
Input Voltage (recommended)	7-12V
Digital I/O Pins	14 (6 PWM output)
Analog Input Pins	6
DC Current per I/O Pin	40 mA
Flash Memory	32 kB
SRAM	2 kB
EEPROM	1 kB
Bootloader memory usage	0.5 kB
Clock Speed	16 MHz

Digi's XBee Series 1 radio modules use the IEEE 802.15.4 networking protocol. It allows them to transmit data in a point-to-point, peer-to-peer or point-to-multipoint network architecture. Modules utilize one of the first 12 transmission channels of the 2.4 GHz ISM band and the configured channel can be changed on the fly. The 802.15.4 standard specifies RF

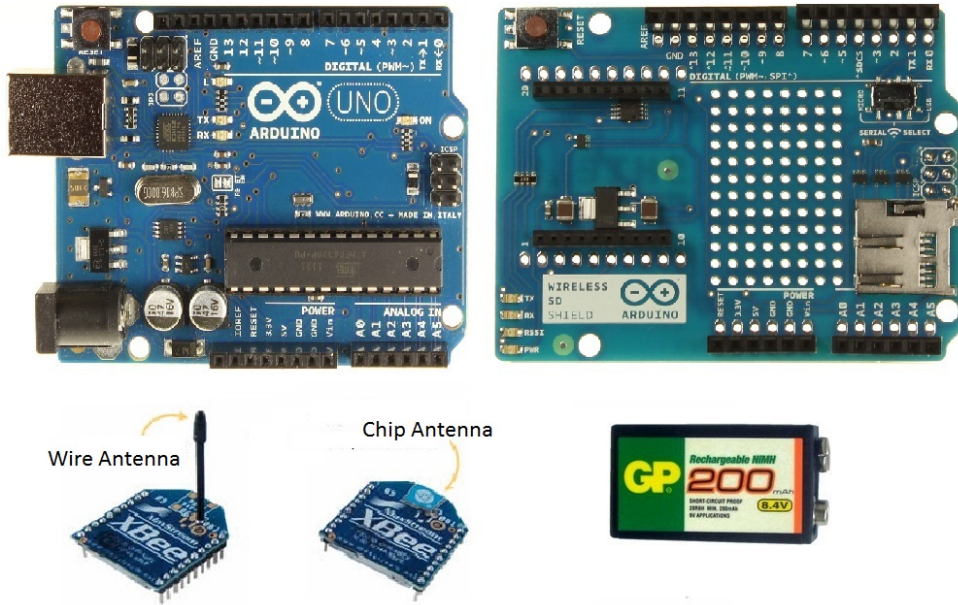


Figure 4.1: Sensor node elements

baud rate of 250 Kbps at 2.4 GHz, which is equal to 32 us per byte. The time it takes to transmit a data packet is the sum of the time on air and the time for Carrier Sense Multiple Access-Collision Avoidance (CSMA-CA) retries. The process that an XBee radio senses the carrier channel to make sure air waves are clear before the transmission is called Clear Channel Assessment (CCA) [15]. If a radio senses strong enough activity on the channel, it incurs a random delay. Next, it tries again with another CCA. This process is repeated up to 4 times. Best case and worst case times needed for transmission after addition of CSMA-CA steps are given in eqn. (4.1). If the worst case time elapses, the XBee module cancels the transmission and sends a CCA error to the connected control unit.

$$\begin{aligned}
 Total\ Time\ on\ Air\ best(k) &= (0.928 + 0.032 * k) ms \\
 Total\ Time\ on\ Air\ worst(k) &= (9.76 + 0.032 * k) ms
 \end{aligned}
 \tag{4.1}$$

An XBee module communicates to a control unit through an asynchronous serial port using Universal Asynchronous Receiver/Transmitter (UART) interface. The pins of an XBee RF module are connected to a master device having a UART interface as shown in Figure 4.2. Serial communication depends on the two UART compatible interfaces to be configured with same settings. Those settings are baud rate, parity, start and stop bits. In this work, sensor nodes are configured such that serial Baud rate is 57600 bps (the second highest serial communication speed used XBee modules can support), start and stop bits are 1 bit, and data bits are 8 bits.

The serial interface of the XBee module supports two modes of operation. In transparent mode, all UART data received through the data input port of the XBee module is queued

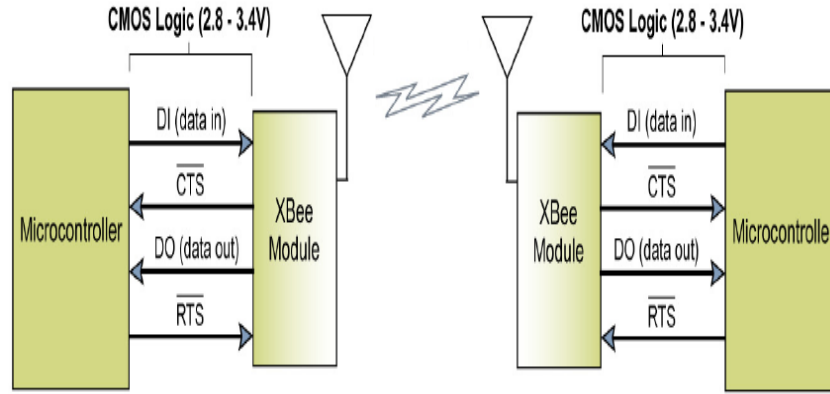


Figure 4.2: Communication data flow of microcontrollers and XBee modules [15]

for RF transmission. After packetization timeout is over or the maximum number of bytes a packet can contain (100 bytes per packet) are received, RF transmission starts. Transmitted data are available at the data ports of receiver XBee modules in the WSN after the transmission time on air mentioned in eqn. (4.1). Then, the control units of the receiver nodes acquire the transmitted data via serial ports. In transparent operation, a distinct command mode is used to reach the internal registers of the XBee module at which specific information such as transmission channel settings, RSSI of last received packet, CCA and acknowledge failures are saved. Alternative of the transparent operation is Application Programming Interface (API) operation. API supports communication with the XBee modules in a frame-based way. In fact, a control unit sends data frames containing destination address and transmission data to the transmitter XBee module together with transmission options. When receiver XBee modules acquire the RF data with API commands, they send data frames containing status packets, source, RSSI and transmission data from received packets to the receiver control units. Since this study considers RSSI-based localization, acquiring RSSI of each transmission in a less complicated way is important. Also, the usage of the frame-based API operation is more advantageous than transparent operation when using serial interface between the MCU and XBee module to change the communication channel. Therefore, API is preferred as the serial interface mode. Moreover, the broadcast destination address (0xFFFF) is selected as the destination address of each transmission. Thus, point-to-multipoint (star) network architecture is used. Transmission and reception API command sets are illustrated in Figure 4.3.

As mentioned at the beginning of the section, NiMH rechargeable 9V 200 mAh batteries are used as the sensor node power supplies. According to information provided by the product manual of GP 9V 200 mAh battery, supply voltage characteristic of the product is illustrated in the Figure 4.4 with respect to discharge time. The product specifications of Duracell and Energizer 9V 200 mAh batteries are also similar. As observed from Figure 4.4, the power supply performance degrades as the discharge rate increases. Since localization schemes to be implemented in this work are RSSI-based, the performance of sensor node battery may have an important effect on the localization performance. It is analyzed experimentally later.

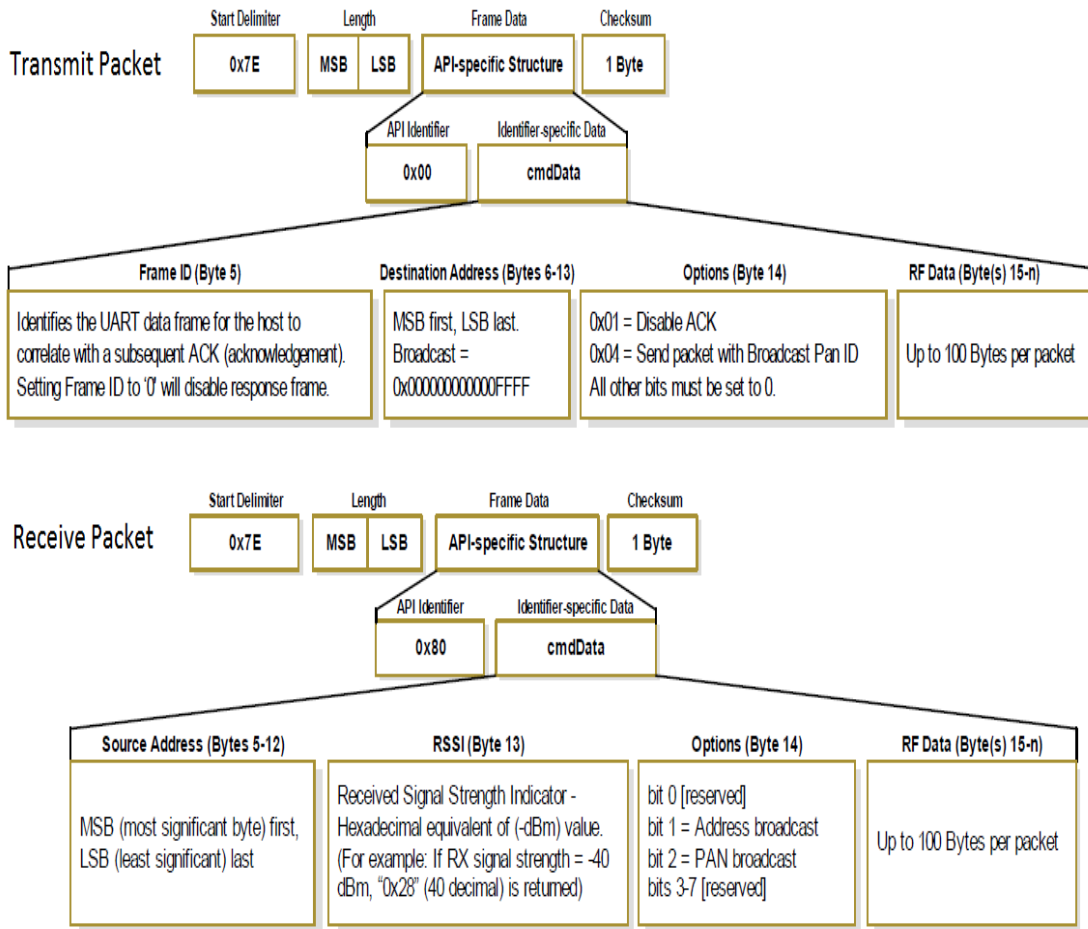


Figure 4.3: UART data frame structure of the API operation [15]

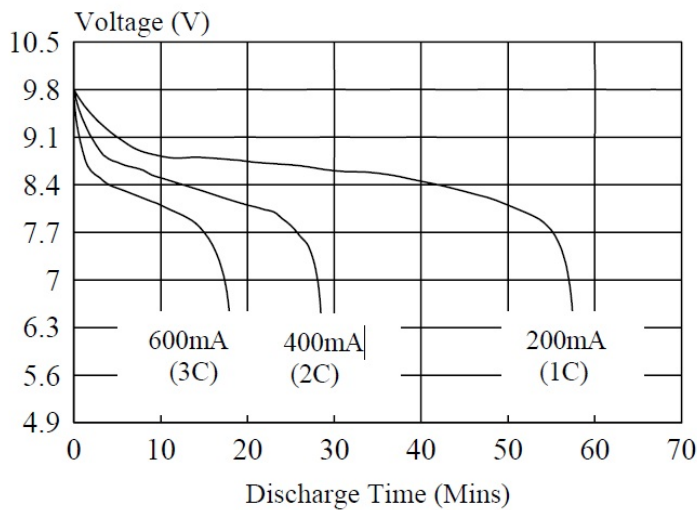


Figure 4.4: Supply voltage versus discharge time [19]

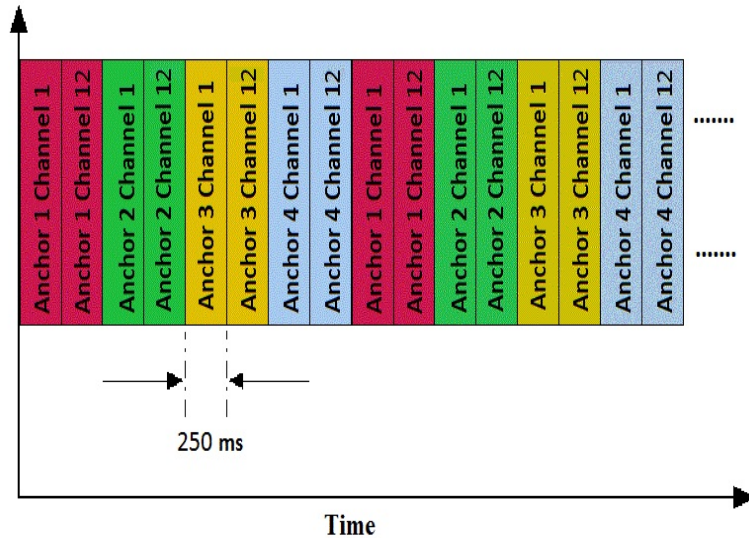


Figure 4.5: Four anchor TDMA scheme

4.1.2 Testbed Scenario Details

Testbeds implemented in this study have many variables. Common features are summarized as follows:

- Three or four anchors are placed at the corners of the localization field to be used in the experiments.
- Node antennas used during experiments are either all wire or all chip antennas.
- Channels 1, 5, 9 and 12 of the 2.4 GHz ISM band are used in the experiments.
- To prevent collusion, the anchor microcontrollers are programmed such that each anchor broadcasts its coordinate at its own time slot. A pair of channels 1, 5, 9 and 12 of the 2.4 GHz ISM band are used at a time. A two-channel time division multiple access (TDMA) scheme used in four-anchor-localization case is illustrated in Figure 4.5. Each anchor microcontroller automatically calculates waiting times according to the period, total number of anchors and anchor order information previously written to its non-volatile memory. Thus, the anchors know their transmission slots after the startup.
- Each anchor is programmed to transmit RSSI measured from previous receptions from other anchors to be used in the model parameter estimation phase.
- According to each transmission of anchor 1, all other anchors reset their timers. Therefore, the loss of synchronization in time is prevented.
- As pointed out in section 4.1.1 Application programming interface (API) commands are used to control the XBee modules. The agent collects data from anchors at channel 1 and

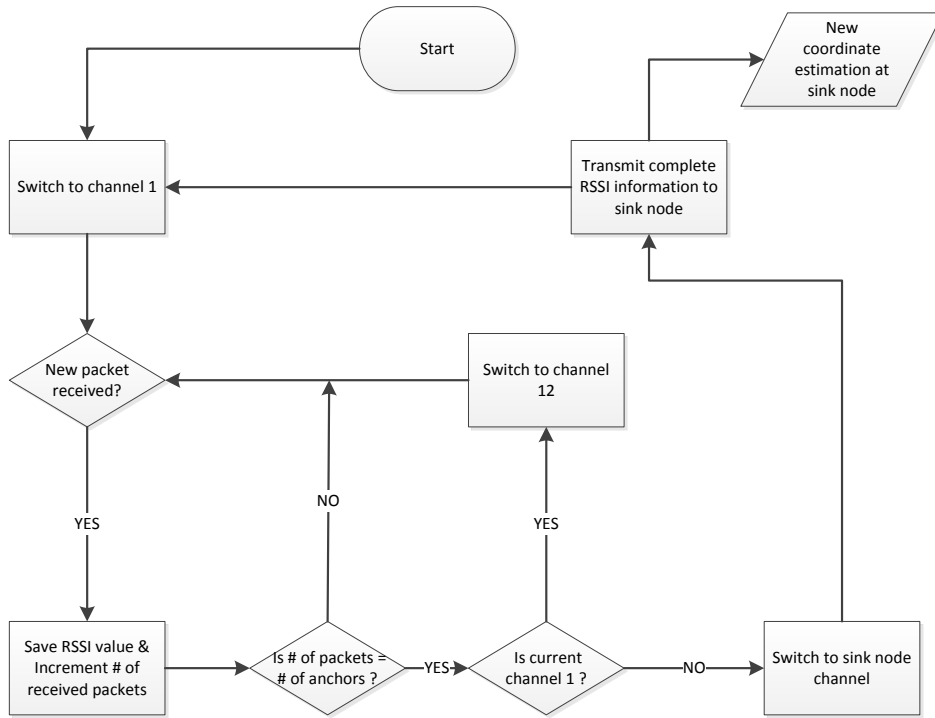


Figure 4.6: Flow chart of the agent algorithm

12 and combines data from all anchors. Then, it transmits those data to a sink node serially connected to a personal computer by using channel 3 of the 2.4 GHz ISM band (selected sink node channel). Flowchart of the agent algorithm is shown in Figure 4.6.

- The sink node (PC) saves the data set received from the agent and calculates the agent coordinates via localization algorithms coded on MATLAB. Therefore, centralized localization is performed.

4.2 Experimental Results

4.2.1 Analyses of the Factors Affecting Localization Performance

4.2.1.1 Experiments about Multichannel Measurements

In this section, the effect of frequency hopping (FH) on the RSSI measurements in the 2.4 GHz ISM band is experimentally analyzed. In the 2.4 GHz ISM band, there are 16 sub-channels available with 5 MHz separations. It is a 75 MHz operational band with carrier frequencies equal to

$$f_m = 2405 + 5(m - 11) [MHz], \quad m = 11, \dots, 26. \quad (4.2)$$

To validate that FH can mitigate fading and decrease related localization errors, extensive data

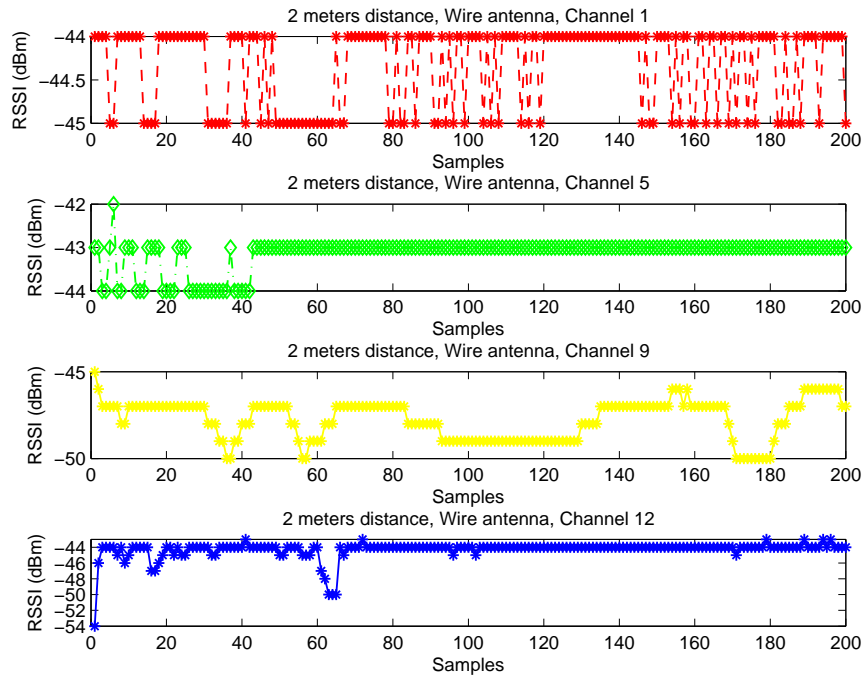


Figure 4.7: Frequency hopping experiment 1

are collected when sensor nodes are working at channels 1,5,9 and 12. Two sensor nodes are placed with two or three meters away from each other and their heights are fixed as one meter. Experiments are conducted at the different coordinates of a hallway which is 7 m in width, 7 m in length, and 5 m in height with three park benches at the corners and some asymmetrical walls.

As observed in Figures 4.7, 4.8, 4.9 and 4.10, different channels provide different mean RSSI values. The mean of the measured powers are different for the sensor nodes communicating with different radio channels. For instance, when the distance between sensor nodes with wire antennas is 2 meters, channel 5's mean power is around -43 dBm while channel 9 mean power is around -47 dBm. Moreover, when the distance between sensor nodes with chip antennas is 3 meters, channel 1's mean power is around -54 dBm while channel 12 mean power is less than -61 dBm.

It is significant to observe that the usage of multiple carrier frequencies provides RSSI measurements with different characteristics. Thus, more reliable data can be obtained by processing RSSI samples from different channels. Experiments conducted under various conditions to analyze effects of multichannel transmissions on the accuracy of the localization algorithms are to be provided in the localization experiments section.

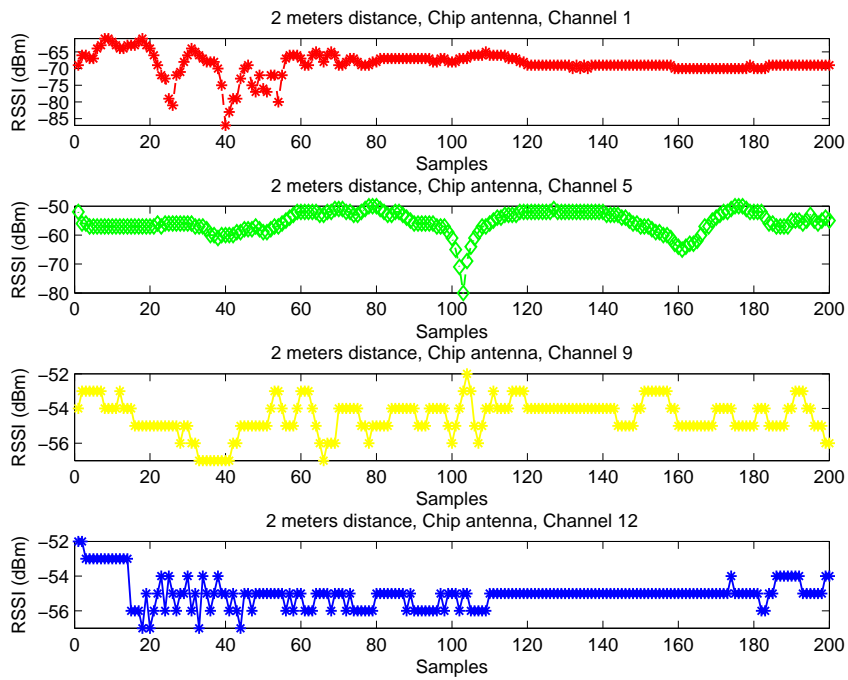


Figure 4.8: Frequency hopping experiment 2

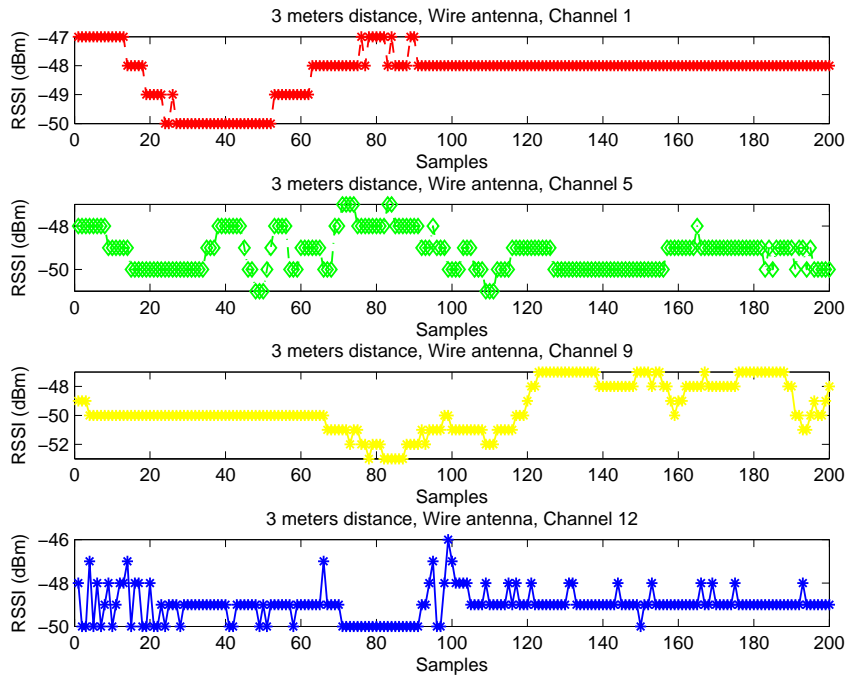


Figure 4.9: Frequency hopping experiment 3

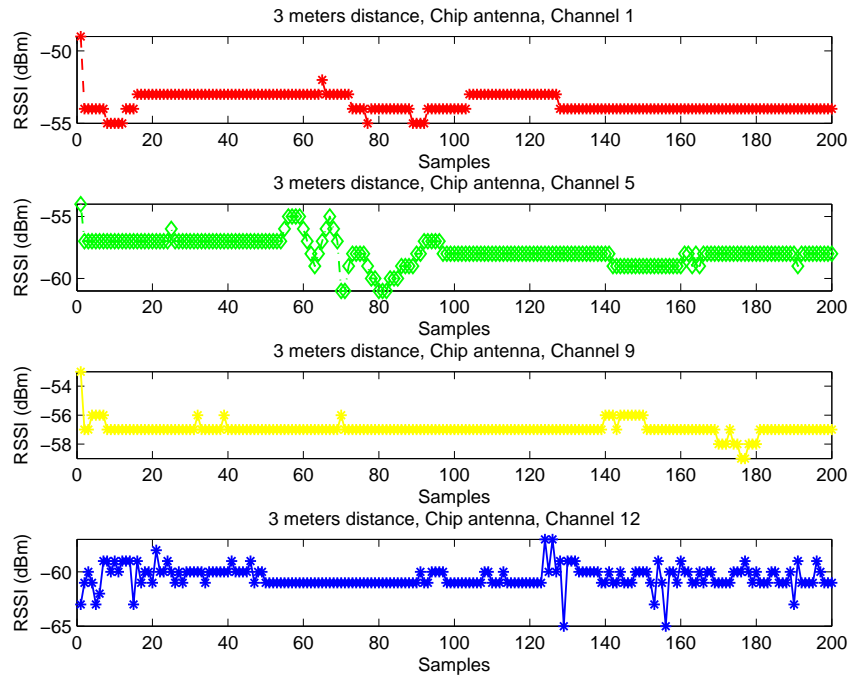


Figure 4.10: Frequency hopping experiment 4

4.2.1.2 Experiments about Propagation Model Parameters

In a real scenario, the system model parameters, path loss exponent and reference power, may depend on the environmental conditions. In this section, variation of these two parameters in time which may affect the localization accuracy is examined.

To begin with, the real time power consumption of the sensor node is measured using a current probe and a 9-volt power supply. The sensor node microcontroller is programmed to send API commands to the XBee radio so as to transmit data packets with a 100 ms period. The steady-state current drawn from power supply is measured around 70 mA and the mean current usage is found to be roughly 130 mA. Thus, average power consumption is around 600 mW which is high compared to the similar sensor nodes having a power consumption around 50-100 mW. However, there two main reasons of the choice of sensor nodes used in this work. First, the preferred components have relatively shorter lead times and cheaper prices compared to counterparts. Second, sensor nodes obtained with the integration of these components are capable of performing on-the-fly frequency hopping.

Afterwards, the deviation of RSSI as the sensor node battery droops is analyzed. Two sensor nodes with chip antennas are placed at a distance of 3 meters from each other and their heights are fixed as one meter. Also, the azimuth angle of the sensor nodes are set to 0° . The power supplies are fully charged before the start of each set of measurement. One of the XBee modules is set to transmit data with a 100 ms period and then various RSSI measurements are

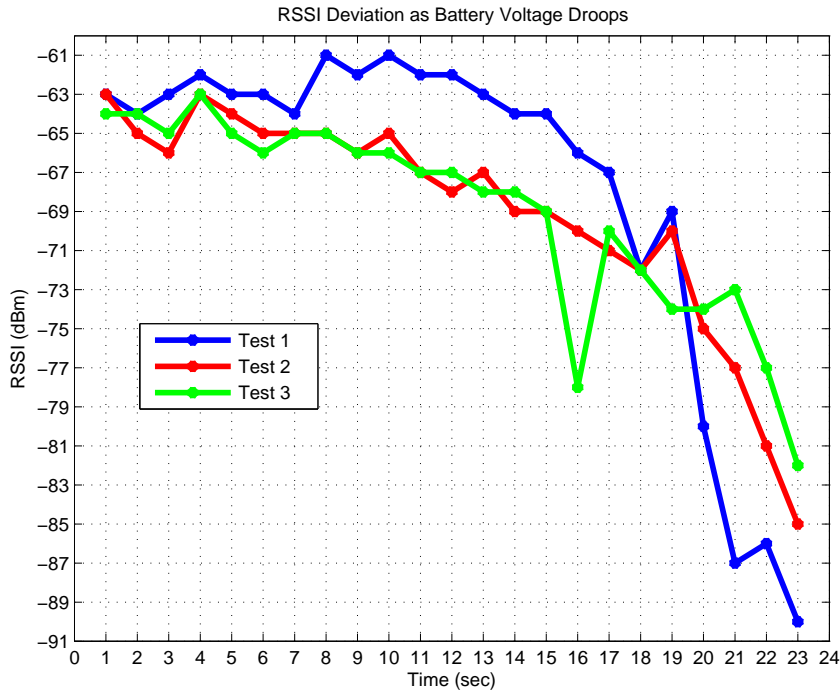


Figure 4.11: RSSI deviation as battery droops in time

taken until nodes are unable to communicate with each other as their batteries run out. The same experiment is conducted in three different indoor environments with some dissimilarities such as multiple desks, chairs and bookshelves. RSSI measurements taken in a second are averaged and these averages are drawn against time for the last 24 seconds of each experiment in Figure 4.11.

According to the results, RSSI samples tend to fluctuate and decrease in time in different ways. Nevertheless, there is a definite pattern of voltage droop in time. Except from the voltage droop, various dynamic factors such as temperature, humidity, changes in the geometry of localization environment or human traffic in the localization area etc. may affect RSSI measurements in time. Therefore, the path loss model parameters, namely reference power and path loss exponent, may also change in time. In other words, the usage of constant model parameters can be one of the various error sources of RSSI-based localization.

In the proposed localization method, range model parameters are updated using the online RSSI values and calibrated according to the recent measurements as explained in Section 3.2.2. To emphasize the importance of the mentioned problem and potential enhancement of proposed approach, a localization experiment analyzing the effects of model parameter estimations on localization algorithms accuracy is conducted. Its details and critical results are to be given in the localization experiments section.

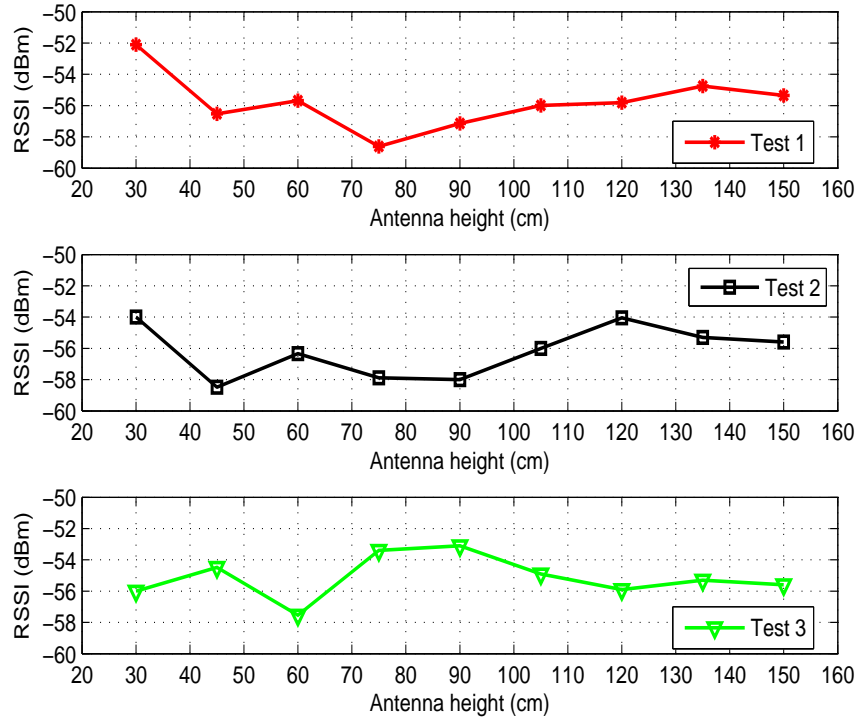


Figure 4.12: Antenna height versus RSSI measurements

4.2.1.3 Experiments about Antenna Performances

Antenna performance is another vital point for indoor RSSI localization. Naturally, WSN nodes are expected to be tiny devices; therefore wide antennas with smooth patterns are not feasible for WSN localization. It is inevitable to use small antennas with non-isotropic gain patterns. Such antennas' performance may differ from device to device for the same manufacturer as illustrated in [14] even when antenna pattern changes due to the objects around are neglected. Antenna height also affects RSSI-based localization. In [27], receiver antenna heights were varied from 0.5 m to 3 m and it was observed that the measured RSSI data were between -51 to -63 dBm. In order to analyze these issues, two different experiments are conducted using wire and chip antennas in a 6m by 5m room with some furniture.

In the first experiment, the effect of the antenna height on RSSI measurements is tested by keeping the height of the anchor as 75 cm and changing the height of the agent with chip antenna from 30 cm to 150 cm when distance between two nodes is 2 meters. Same experiment is repeated for three times when the agent is at different coordinates in a 6 m by 5 m room. As seen in Figure 4.12, measurements are stabilized only after 100 cm. Therefore, it is better to place anchor antennas at least one meter above the ground and below the ceiling to minimize reflections. For instance, experimental data collected via mobile robots at low heights may not be reliable. One should take height effect into account.

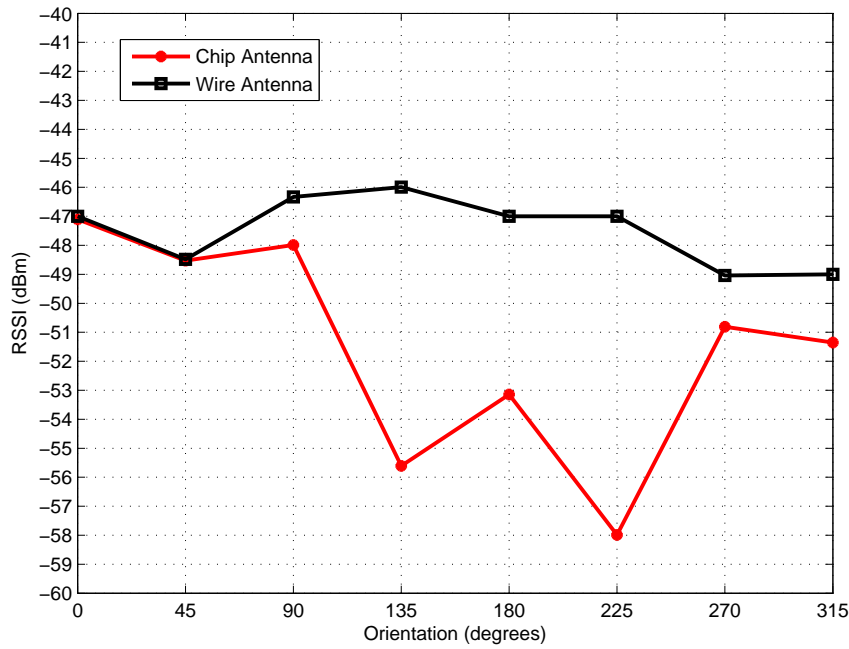


Figure 4.13: Orientation versus RSSI measurements

In the second experiment, the orientation of the sensor node antenna versus RSSI measurements is examined. The anchor is placed 2 meters away from the agent and its orientation is fixed. Node heights (antenna heights) are set as one meter. For each orientation of the agent, 50 samples are taken and averaged. As seen in Figure 4.13, antenna patterns are non-isotropic and different for wire and chip antennas. The received power variation of the wire antenna is around 3 dB. On the other hand, the chip antenna pattern has a variation more than 11 dB. In fact, selection of the more advantageous antenna type depends on the implementation details. For instance, distortion in the gain pattern can be used beneficially so as to determine directions of the agents and to remove errors due to non-isotropic antenna patterns [53], so a chip antenna can be preferred in that approach. However, an antenna performing close to the ideal isotropic antenna is often preferred for RSSI-based WSN localization. Localization experiments about the effects of antenna performances are in order.

4.2.2 Localization Experiments

In this section, RMSE performances of the implemented localization algorithms, namely trilateration, quadrilateration, MDS and MLE, are analyzed. Experiments are conducted in 7 m by 7 m and 6 m by 4 m areas. The anchor microcontrollers are programmed to broadcast their positions using 802.15.4 channel 1 and channel 12 similar to the one illustrated in Figure 4.5. Channel durations are set to 250 ms. During measurements a person walked around the area with a constant speed around (0.5 m/sec) so as to create some multipath effects. It is paid attention not to cause non-line-of-sight (NLOS) conditions during this process. Node heights

Table 4.2: The agent position numbers and the corresponding coordinates for experiment 1

Position number	Agent coordinate
1	(3.5,3.5)
2	(2.0,3.5)
3	(2.0,5.0)
4	(5.0,5.0)
5	(6.0,3.5)

are adjusted to 1 meter in the light of experiments mentioned in section 4.2.1.3. Data from channel 1 only, channel 12 only, maximum of two channels and linear average of two channels are used as inputs to the localization algorithms. For the MLE algorithm, results for the extended multichannel method are also provided. Details of each experiment are as follows.

4.2.2.1 Localization Experiment 1

The purpose of localization experiment 1 is to investigate the effects of the frequency hopping, antenna type and addition of the fourth anchor on the implemented localization algorithms' performances. In the first part of localization experiment 1, three anchors all having wire or chip antennas are placed at the coordinates (0.0,0.0), (7.0,0.0) and (7.0,7.0) of the 7 m by 7 m area. The agent is located at five different positions whose coordinates are (3.5,3.5), (2.0,3.5), (2.0,5.0), (5.0,5.0) and (6.0,3.5). For each agent position, RMSE of the algorithms are calculated by using 150 different agent position estimates. RMSE performances of the implemented algorithms with wire and chip antennas are given in Figures 4.14 and 4.15 with respect to the agent positions. The agent coordinates are enumerated as shown in Table 4.2. From Figures 4.14 and 4.15 many comments are in order.

- Multichannel refinements are capable of increasing the localization accuracy. For instance, the best RMSE results are obtained by MLE with maximum RSSI refinement in the wire antenna case. Its RMSE is below 1 meter at agent positions (3.5,3.5), (2.0,3.5) and (5.0,5.0). For the chip antenna case, the MLE with the extended multichannel method has the best performance. It provides RMSE less than 0.5 meter at the agent coordinates (2.0,3.5) and (5.0,5.0). Therefore, multichannel refinements can be used to improve the performance of RSSI-based indoor WSN localization. However, there is not a clear result showing that one method is dominant. Different refinement methods have better results for different algorithms and antenna types. This is probably due to the statistically inadequate number of data used in obtaining numerical results.

- The type of antenna evidently influences the RMSE performance in parallel to previous work mentioned in Section 4.2.1.3. For instance, RMSE of the MLE is four times more with three chip antennas than with three wire antennas when the agent is at (5.0,5.0). However, with the usage of refinements performance differences between chip and wire antennas decrease in other four agent locations. Therefore, it can be concluded that multichannel refinements

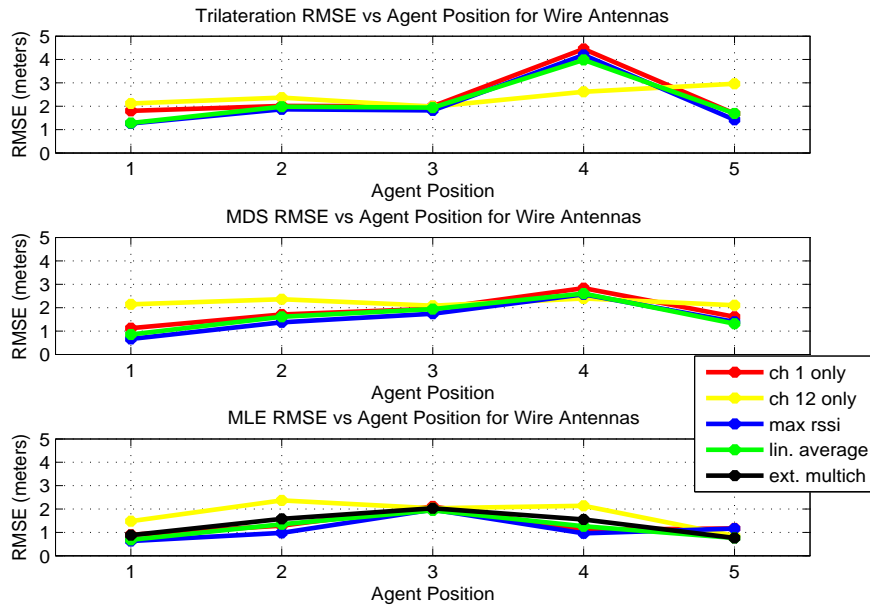


Figure 4.14: RMSE performances of algorithms with three wire antenna anchors

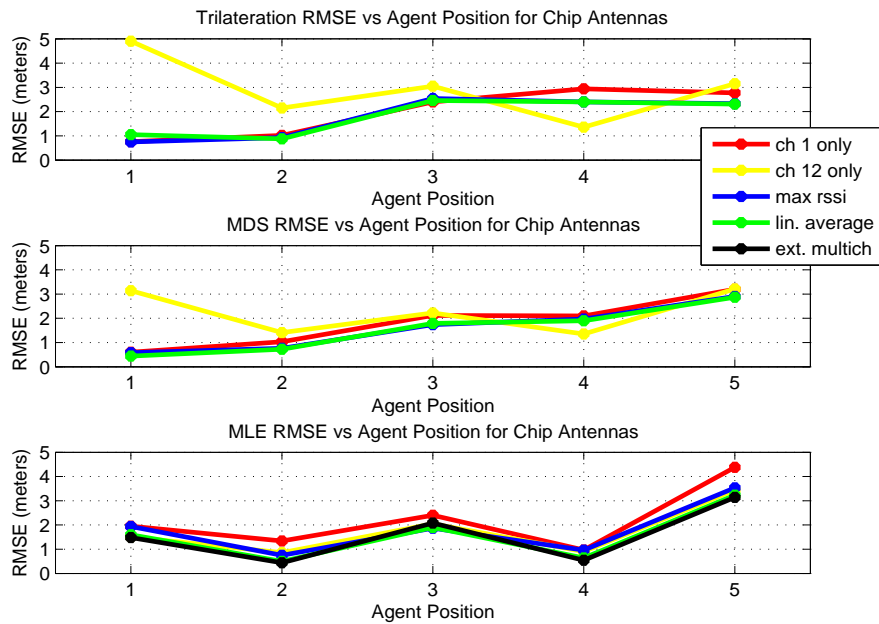


Figure 4.15: RMSE performances of algorithms with three chip antenna anchors

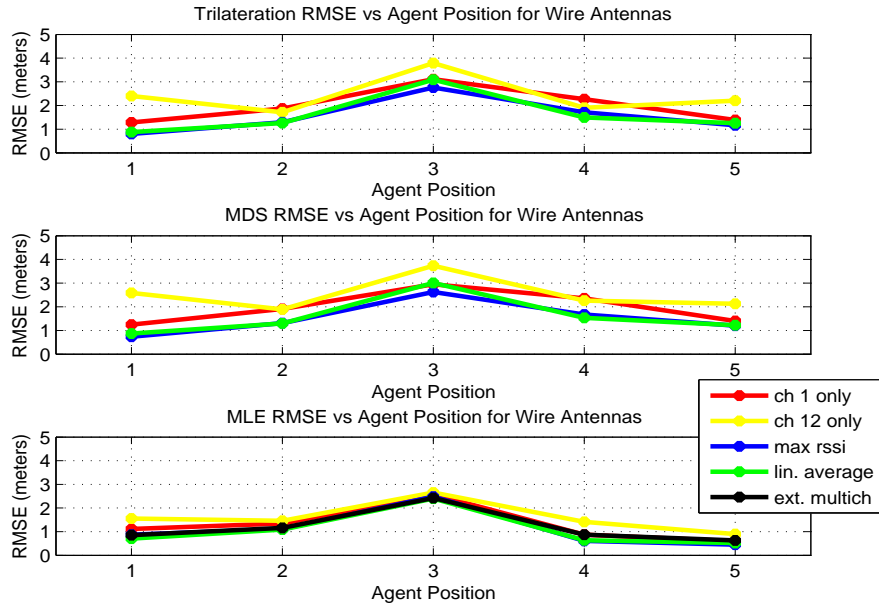


Figure 4.16: RMSE performances of algorithms with four wire antenna anchors

reduce the antenna pattern dependency of RSSI-based indoor WSN localization.

- The MLE algorithm outperforms the MDS and trilateration when the agent is close to the edges of the localization area. For instance, MLE with multichannel refinements can provide RMSE less than 0.6 meter, while trilateration and MDS errors are around 2 meters under the same conditions. On the other hand, both trilateration and MDS with multichannel refinements perform well when the agent is around the middle of localization area and MDS is better than trilateration in most cases.

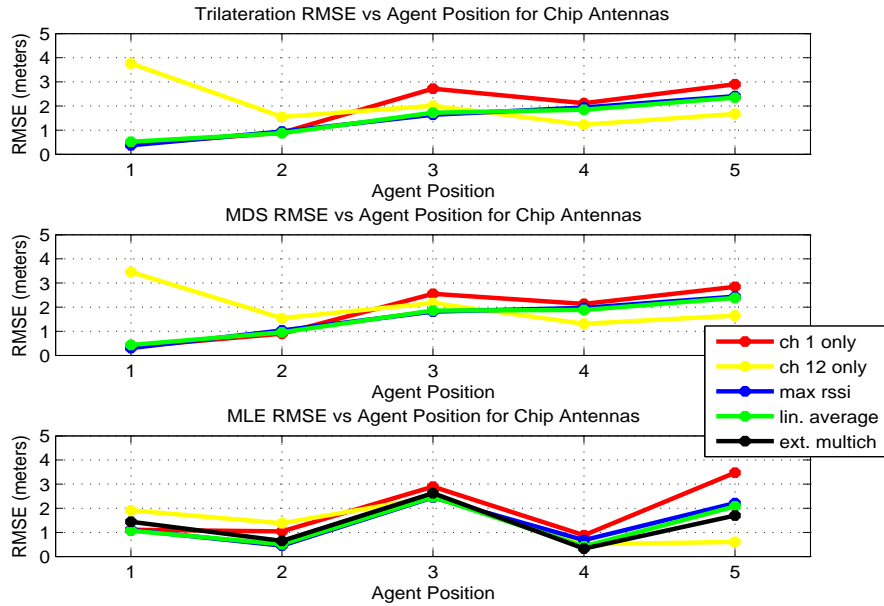


Figure 4.17: RMSE performances of algorithms with four chip antenna anchors

In the second part of the localization experiment 1, the fourth anchor located at the coordinate (7,0) is added to the localization scheme. In Figure 4.16 and 4.17, the effects of the addition of the fourth anchor in chip and wire antenna cases are observed. Following conclusions are drawn.

- Although placement of the anchors becomes symmetrical with the addition of the fourth anchor, RMSE of the algorithms does not decrease significantly in all cases. Moreover, the fourth anchor affects algorithms using chip antenna less compared to wire antenna. According to comparisons of the results at five agent positions shown in Figures 4.15 and 4.17, RMSE of the four-chip-antenna-anchor case is at most 15 % better than RMSE three-chip-antenna-anchor case. The same percentage increases up to 80 % in wire antenna cases as observed from Figures 4.14 and 4.16

In Figure 4.18, bias performances of MLE with different refinements versus the agent coordinates in the three-anchor-case are given.

- According to the results, the worst bias performances in both wire and chip antenna cases are obtained when frequency hopping is not used.
- Although all results are biased, MLE with refinement methods have a lower bias level. For instance, MLE with extended multichannel refinement can decrease the coordinate biases in the chip antenna case around zero when the agent is at (2.0,3.5) and (5.0,5.0). In the wire antenna case, MLE with maximum RSSI refinement can decrease the bias of x and y coordinates to one third of single channel's when the agent is at (2.0,3.5). Again, successes of the refinements are seems to be random.

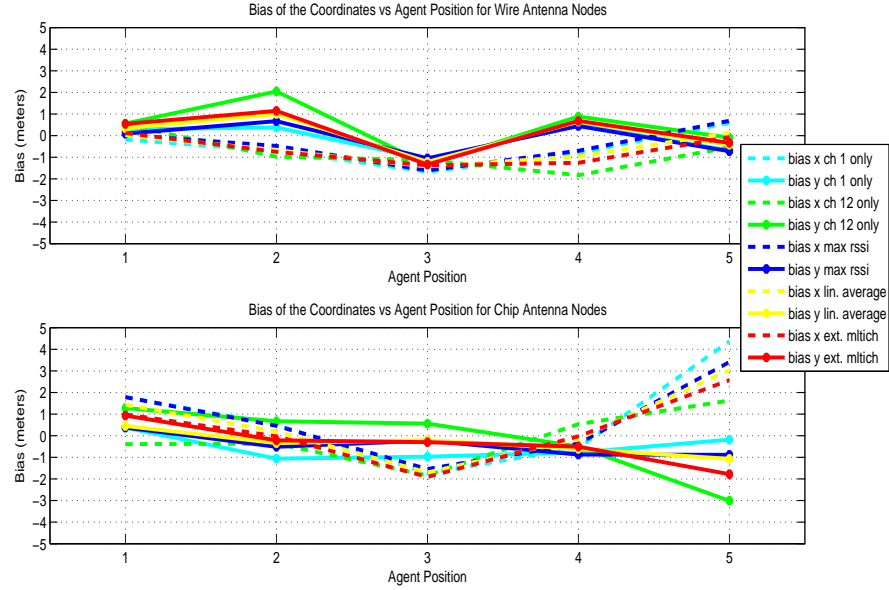


Figure 4.18: Bias performance of MLE with different refinements methods in three anchor case

Table4.3: The agent position numbers and the corresponding coordinates for experiment 2

Position number	Agent coordinate
1	(3.4,2.5)
2	(3.0,1.0)
3	(2.0,2.1)

4.2.2.2 Localization Experiment 2

The purpose of localization experiment 2 is to investigate the effects of antenna orientation on the implemented localization algorithms' performances. Each node used in this experiment has a chip antenna. To observe how antenna orientation affects localization accuracy, the azimuth angle of the agent is set to 0° and 225° since the largest RSSI difference for a chip antenna is measured at 0° and 225° antenna orientations as shown in Figure 4.13.

In the first part of the localization experiment 2, three anchors are placed at the coordinates (1.0,0.0), (6.0,1.0) and (6.0,4.0) of a room 6 m in width, 4 m in length, and 3 m in height with multiple chairs, a table and a bookshelf. The agent is located at three different positions whose coordinates are (3.4,2.5), (3.0,1.0) and (2.0,5.1). For each agent location, RMSE of the algorithms are calculated by using 150 different agent position estimates. Each set of experiments is conducted twice when agent antenna orientation is 0° and 225° . RMSE performances of the implemented algorithms with 0° and 225° chip antenna orientations are given in Figures 4.19 and 4.20 with respect to the agent positions. The agent coordinates are enumerated as shown in Table 4.3. The notable observations are as follows.

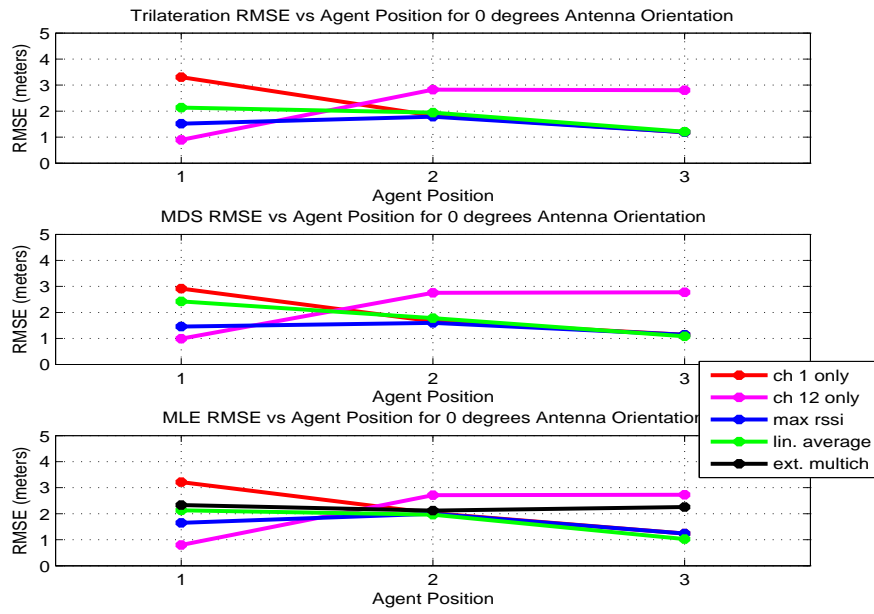


Figure 4.19: RMSE performances of algorithms with three 0 degree orientation chip antenna anchors

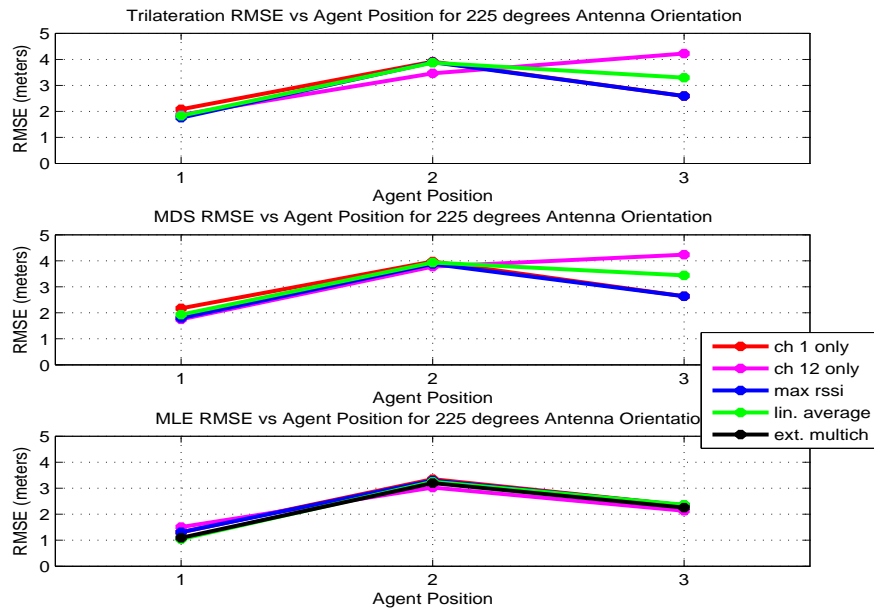


Figure 4.20: RMSE performances of algorithms with three 225 degrees orientation chip antenna anchors

- According to the results, antenna orientation may significantly affect the RMSE performance. In fact, this result supports the non-isotropic gain pattern problem mentioned in Section 4.2.1.3. In the 0° orientation case, MLE with linear average refinement provides the best performance. For instance, MLE with linear average refinement can decrease the RMSE by 25 % compared to the single channel RMSE when the agent is at (3.0,1.0). In the 225° orientation case, MLE performance is better than other algorithms in all conditions and the usage of extended multichannel refinement results in minimum RMSE.

- The benefit of multichannel transmissions is also observed in this experiment. In fact, algorithms with multichannel refinements perform better than at least one of the channel 1 and channel 12 performances. However, the improvements on RMSE performances are less explicit in localization experiment 2. The reason of this is probably the different localization area used in this experiment. It has different dissimilarities and its size is less than half of the one in localization experiment 1.

In the second part of the localization experiment 2, the fourth anchor located at the coordinates (0,4) is added to the localization scheme. In Figure 4.21 and 4.22, the effects of the addition of the fourth anchor in 0° and 225° antenna orientations are illustrated. Also, bias performances of MLE with different refinements versus the agent coordinates in three-anchor-chip-antenna-case are illustrated in Figure 4.23. Following conclusions are drawn.

- In this experiment, the addition of the fourth anchor has different effects compared to experiment 1. In fact, RMSE with four anchors is at most 30 percent better than RMSE with three anchors when refinement methods are used. The reason lying behind this can be the fact that multipath propagation effects are different in the localization area used in experiment 2.

- In both 0° and 225° antenna orientations, linear average and maximum RSSI refinements provide the best results. Also, the worst bias performance in 0° antenna orientation is obtained when using only channel 1 measurements and the worst bias performance in 225° antenna orientation is obtained when using only channel 12 measurements. In the lights of the results, it is concluded that the usage of non-isotropic antennas may degrade the performance of RSSI-based localization.

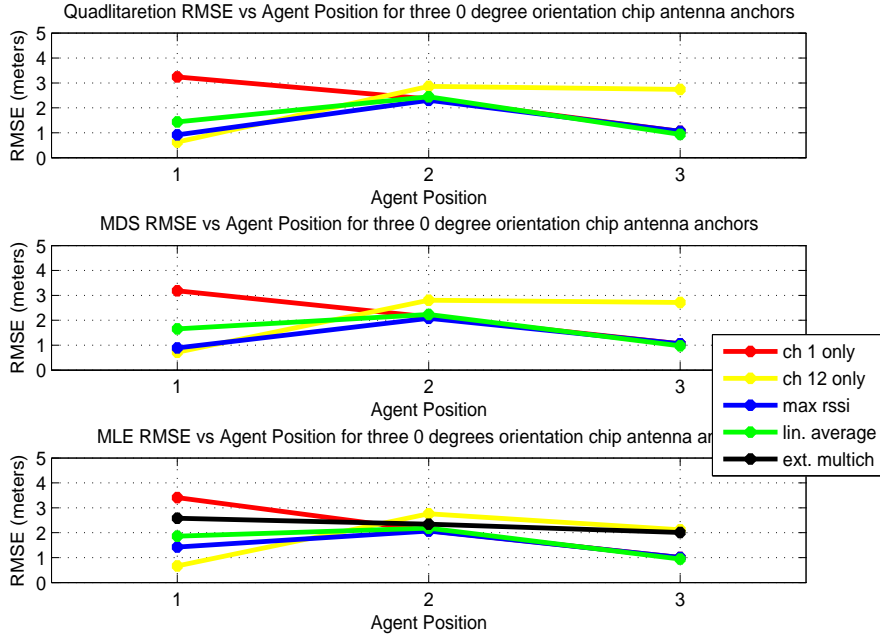


Figure 4.21: RMSE performances of algorithms with four 0 degree orientation chip antenna anchors

4.2.2.3 Localization Experiment 3

The purpose of localization experiment 3 is to investigate the effect of estimating path loss model parameters. In the first two experiments, channel durations are set to 250 ms. Although 150 different measurements taken for each agent position, batteries of the sensor nodes did not droop significantly and affect RSSI measurements as illustrated in Figure 4.11. In order to observe the effect of battery droops quickly, transmission periods of anchors are set to 25 ms and only channel 1 of the 2.4 GHz ISM is used. Measurements are taken in a 7 m by 7 m area using three anchors and one agent all with chip antennas. The anchors are located at coordinates (0,0), (7,0), (7,7). In the first part of the experiment, the agent is located at (2.0,5.0) and at (3.5,3.5) in the second part. For each agent location, average of collected RSSI between sensor nodes in one second and RMSE of the algorithms are provided in Figures 4.24 and 4.26. RMSE of the algorithms calculated using 40 position estimates obtained during one second.

In Figure 4.24, how the estimating path loss parameters in time affects the localization accuracy is illustrated when the agent is located at (2.0,5.0). As the sensor node batteries droop, RMSE of proposed MLE algorithm, which estimates PLE and P_0 using measurements between the anchors and utilizes recent PLE and P_0 estimates, can be less than 1 meter while RMSE of the MLE algorithm using constant model parameters are around 7 meters. Accuracy of the MDS and trilateration are also around 3 meters under the same conditions. Moreover, proposed method can outperform the other algorithms when only P_0 is estimated. PLE and

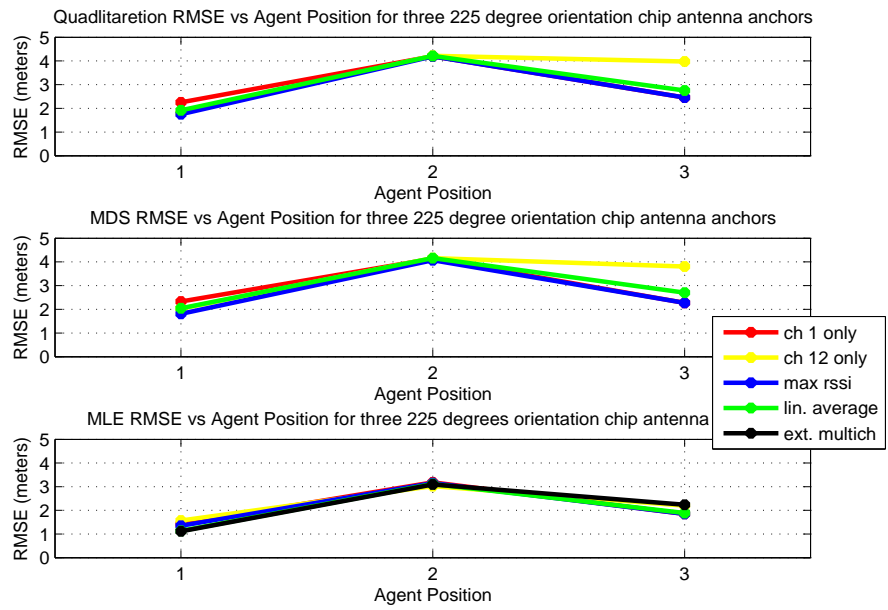


Figure 4.22: RMSE performances of algorithms with four 225 degrees orientation chip antenna anchors

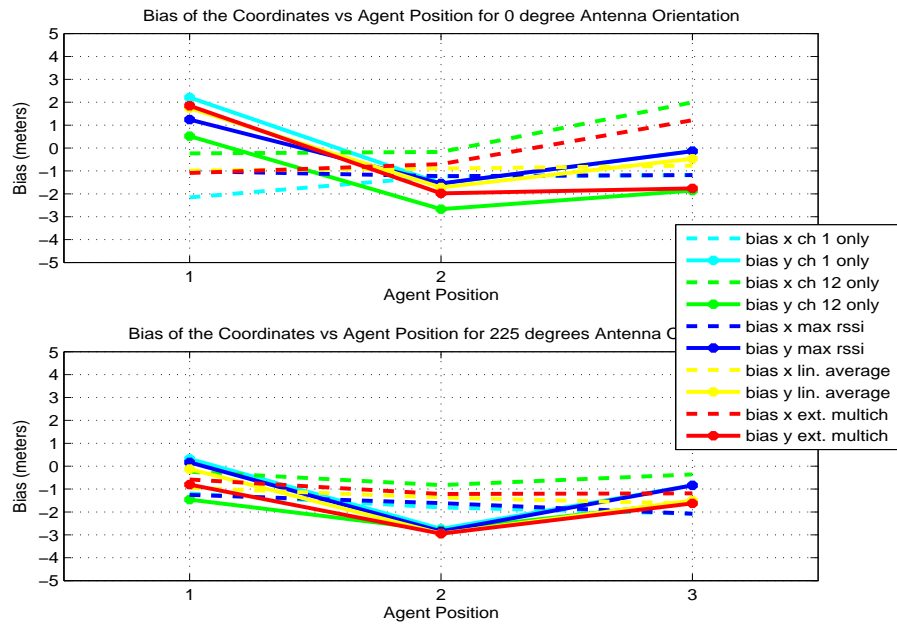


Figure 4.23: Bias performance of MLE with different refinements methods in three anchor case

P_0 estimates are shown Figure 4.25 with respect to time. The oscillations in estimates are resulted from the unexpected variations in the RSSI measurements. In other words, PLE and P_0 estimates for each second model the localization environment better.

In Figure 4.26, results when the agent is located at (3.5,3.5) are given. Similar to previous case, proposed method can achieve sub-meter accuracy while MLE algorithm using constant model parameters has RMSE around 5 meters. Accuracy of the MDS and trilateration are also between 4 and 5 meters under the same conditions. Again, proposed method can outperform the other algorithms when only P_0 is estimated. PLE and P_0 estimates with respect to time are also shown Figure 4.27.

In the light of the experimental results mentioned, following conclusions are drawn.

- Variation of the RSSI measurements due to battery voltage droops is just a case illustrated experimentally in this study, however there exist many other clarified or unknown dynamic factors causing similar variations in indoor RSSI measurements as mentioned in [7]. Therefore, it can be concluded that proposed approach may decrease RMSE significantly when RSSI measurement characteristics in a indoor WSN change in time.
- Since RMSE performance of the MLE with P_0 estimation is comparable to the MLE with P_0 and PLE estimation, former approach can be preferred to reduce to complexity of and power consumption of the algorithm. In that case, only 1-D grid search for P_0 is applied and one AR-1 filter is used.

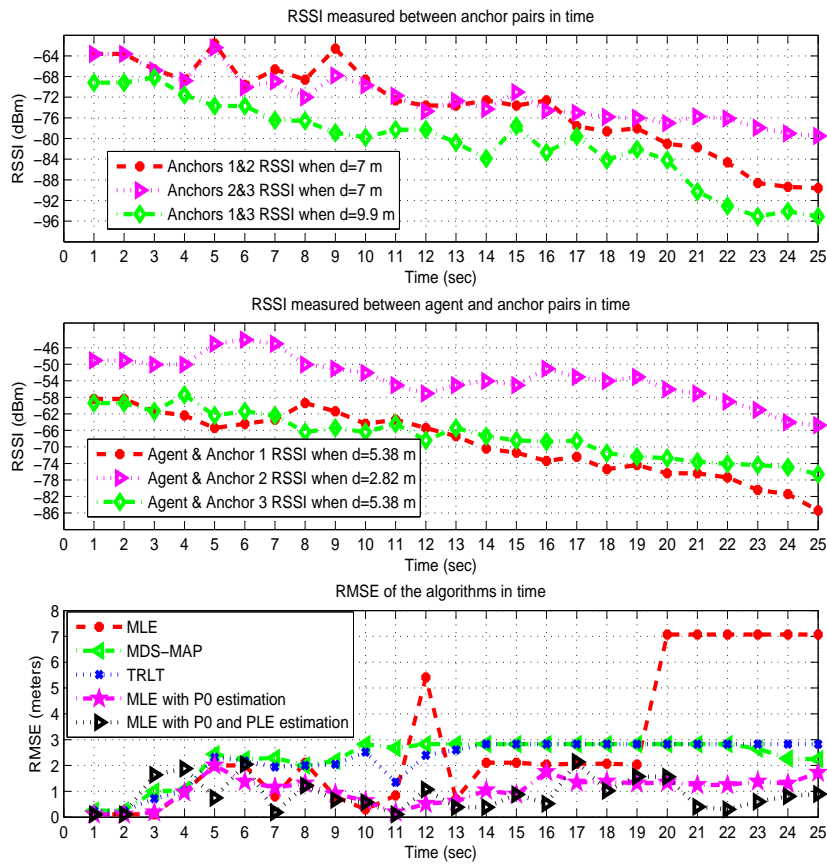


Figure 4.24: Measured RSSI between sensor node pairs in time and RMSE of the algorithms when the agent is at (2.0,5.0)

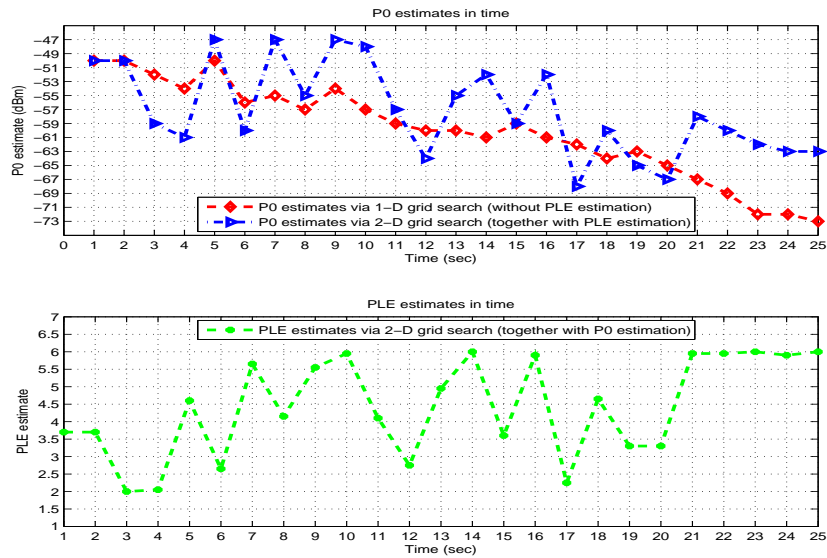


Figure 4.25: Estimated P_0 and PLE values when the agent is at (2.0,5.0)

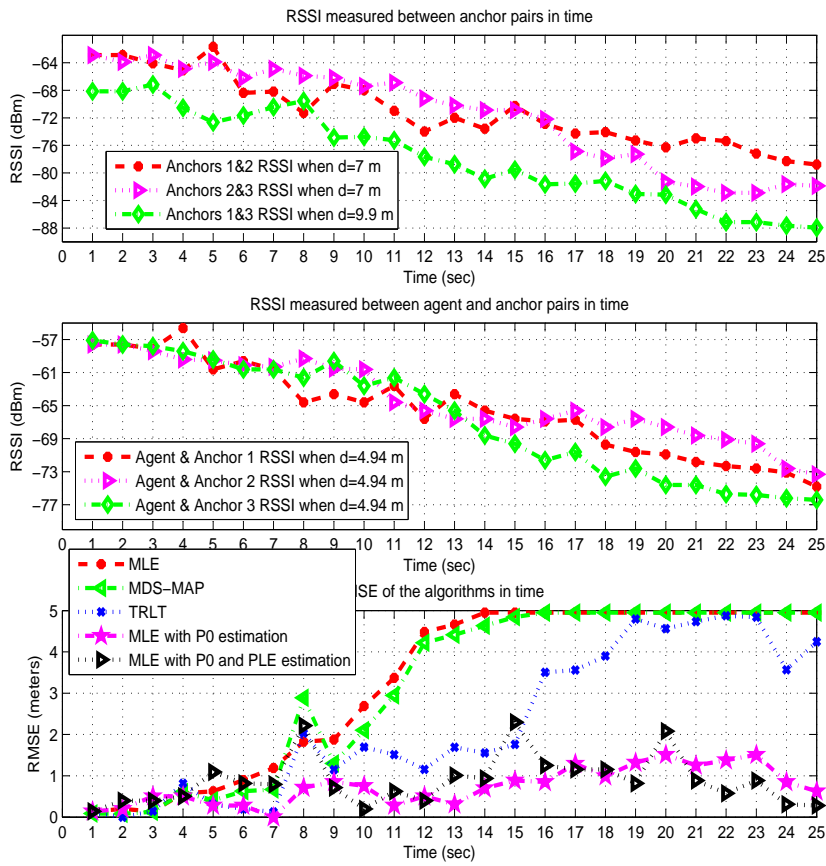


Figure 4.26: Measured RSSI between node pairs in time and RMSE of the algorithms when the agent is at (3.5,3.5)

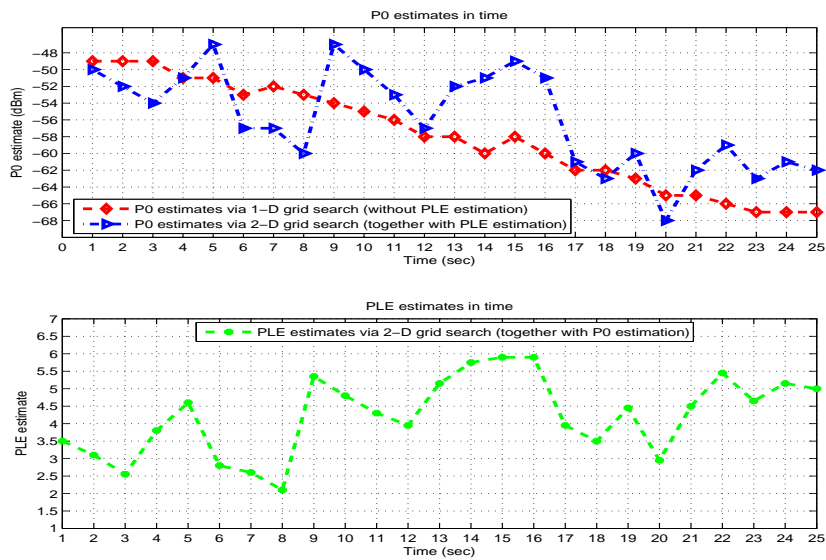


Figure 4.27: Estimated P_0 and PLE values when the agent is at (3.5,3.5)

CHAPTER 5

CONCLUSION

In this study, RSSI-based localization is investigated in sparse-anchor-deployment indoor environments. Multipath propagation, dynamical variations in propagation model parameters and antenna patterns which are three of many potential error sources of indoor RSSI-based localization, are experimentally analyzed. Possible enhancements such as the usage of multichannel measurements and real-time propagation parameter estimation are examined to minimize the effects of mentioned problems.

A multichannel maximum-likelihood estimation (MLE) algorithm using both multichannel measurements and real-time propagation parameter estimation is proposed and implemented in different environments together with some existing localization algorithms. In the light of the experimental results, a number of significant conclusions are drawn.

To begin with, it is validated that multichannel refinement methods, namely linear average, maximum RSSI and extended multichannel, are capable of increasing localization accuracy in indoor RSSI-based localization. In fact, refinements methods may mitigate performance differences caused by unpredictable antenna patterns and the number of available anchors, however different refinement methods have better results for different algorithms and antenna types. Also, it is shown that the usage of constant model parameters may become one of the various error sources of RSSI-based localization. By using real-time propagation parameter estimation, RMSE of the algorithms are decreased significantly when RSSI measurement characteristics change in time. The proposed MLE algorithm provides the best performance among the implemented algorithms by achieving sub-meter accuracy more frequently. Improvements in bias performance are also observed. In addition to these, the importance of antenna types and elevations of sensor nodes for RSSI-based localization are exhibited. It is shown that non-ideal antenna patterns and inadequate heights of nodes may decrease the localization accuracy significantly.

The usage of multichannel refinements and addition of fourth anchor improved localization performance of the algorithms similarly in simulation and experimental results. Moreover, the proposed MLE algorithm provided the best performance in both. Different results are also observed. For instance, the usage of extended multichannel refinement always outperformed the others during simulations, but this situation is not observed experimentally. Moreover,

RMSE of the algorithms changes more rapidly when the agent location is changed in experimental results. Mentioned results are probably due to the statistically inadequate number of agent positions used in obtaining numerical results. Besides, differences between the results of testbed experiments may be explained with the unique multipath characteristics of the testbed environments and other unclarified dynamic parameters.

As a future work, RSSI-based indoor tracking may be investigated in depth and implemented on a testbed. Moreover, the effects of centralized and distributed collaboration on low-anchor-density localization may be examined.

APPENDIX A

CDF OF RMSE AND COORDINATE BIAS OF USED ALGORITHMS

In this chapter, the details of information provided in section 3.3 with Tables 3.1, 3.2, 3.3 and 3.4. In fact, CDF of RMSE and coordinate bias of implemented algorithms in different simulation scenarios are given in Figures A.1, A.2, A.3, A.4, A.5, A.6, A.7, A.8, A.9, A.11, A.11 and A.12.

First, CDFs when three or four anchors are used in case of the noise samples are Gaussian distributed with mean=0 dB and standard deviation=2 dB are provided. Next, the noise samples are Gaussian distributed with mean=0 dB and standard deviation=4 dB cases are given.

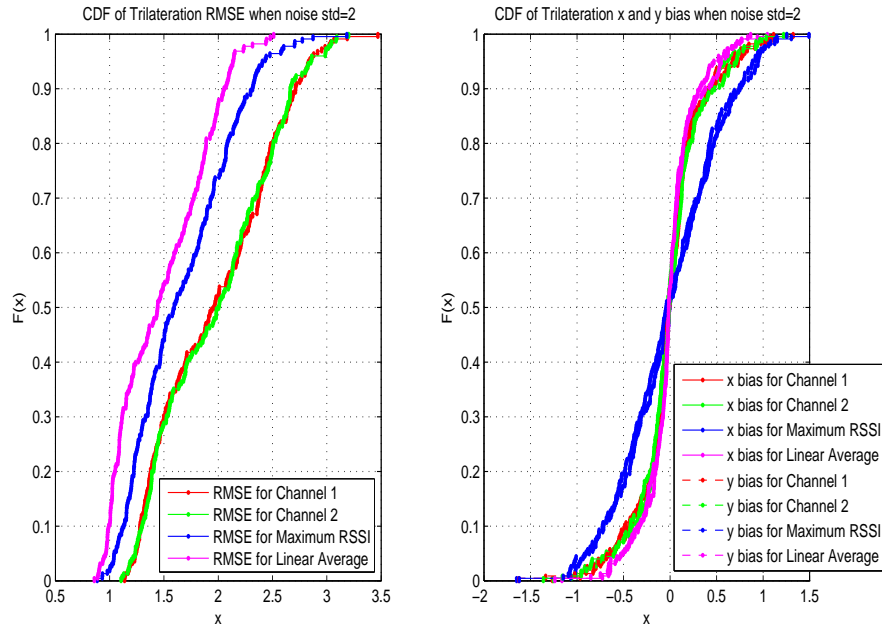


Figure A.1: CDF of Trilateration RMSE and Bias in 3 anchors with error std=2 case

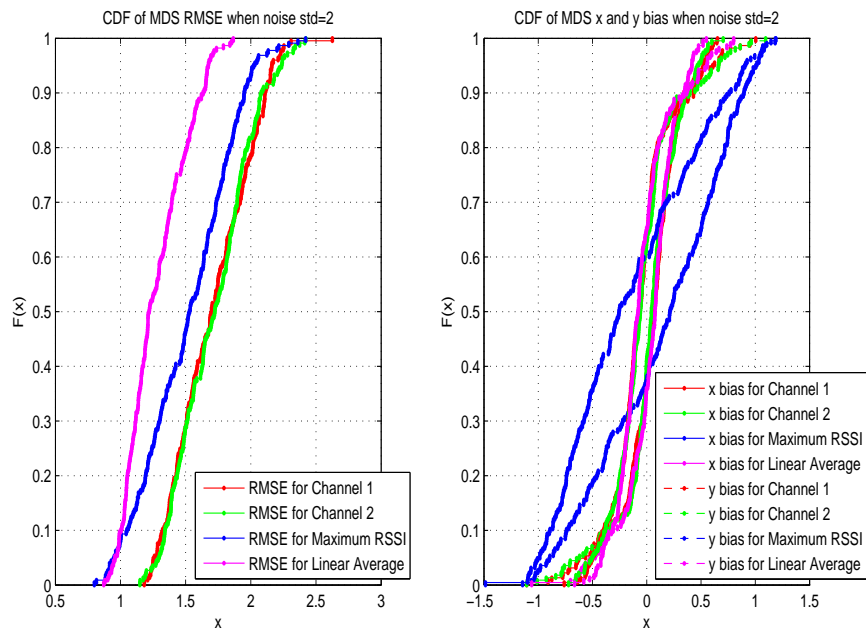


Figure A.2: CDF of MDS RMSE and Bias in 3 anchors with error std=2 case

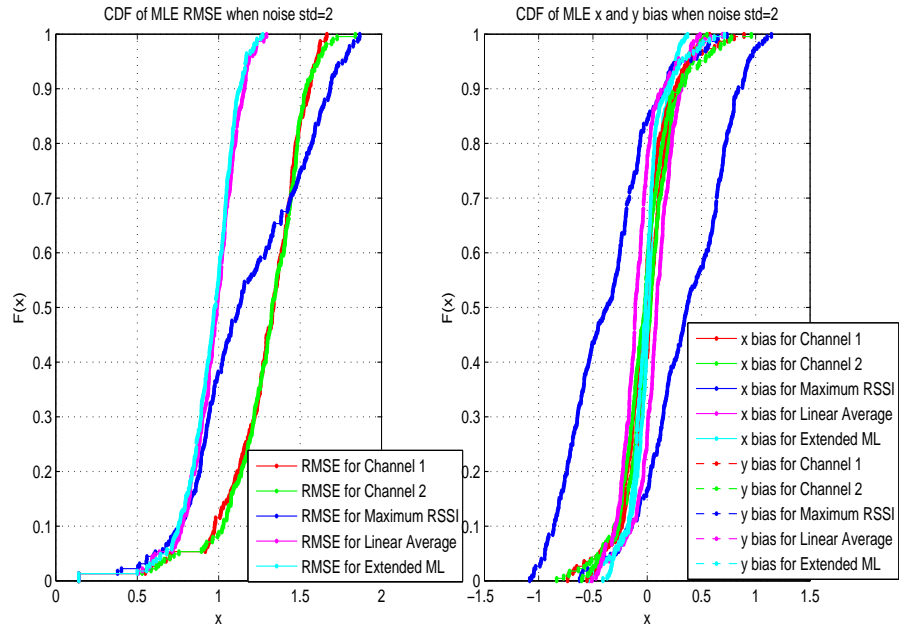


Figure A.3: CDF of MLE RMSE and Bias in 3 anchors with error std=2 case

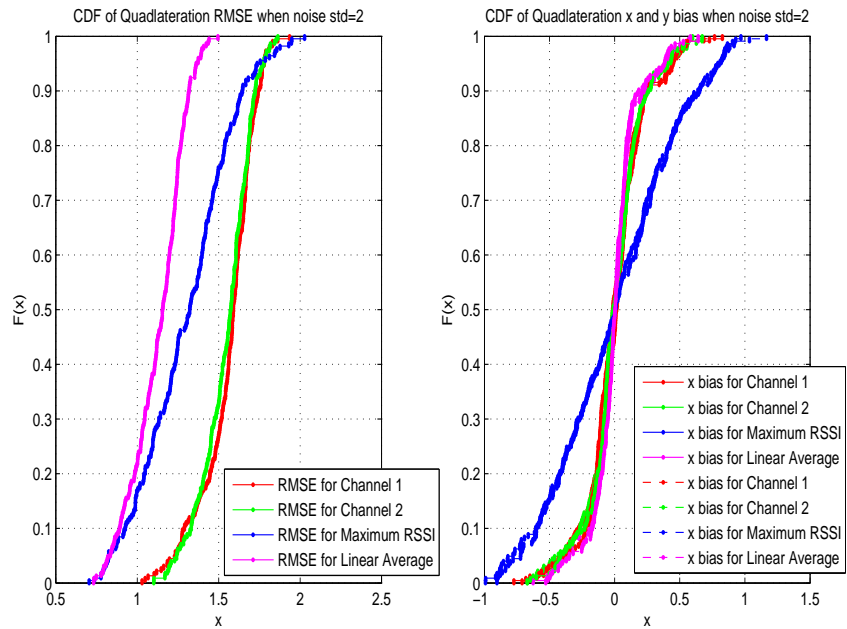


Figure A.4: CDF of Quadlateration RMSE and Bias in 4 anchors with error std=2 case

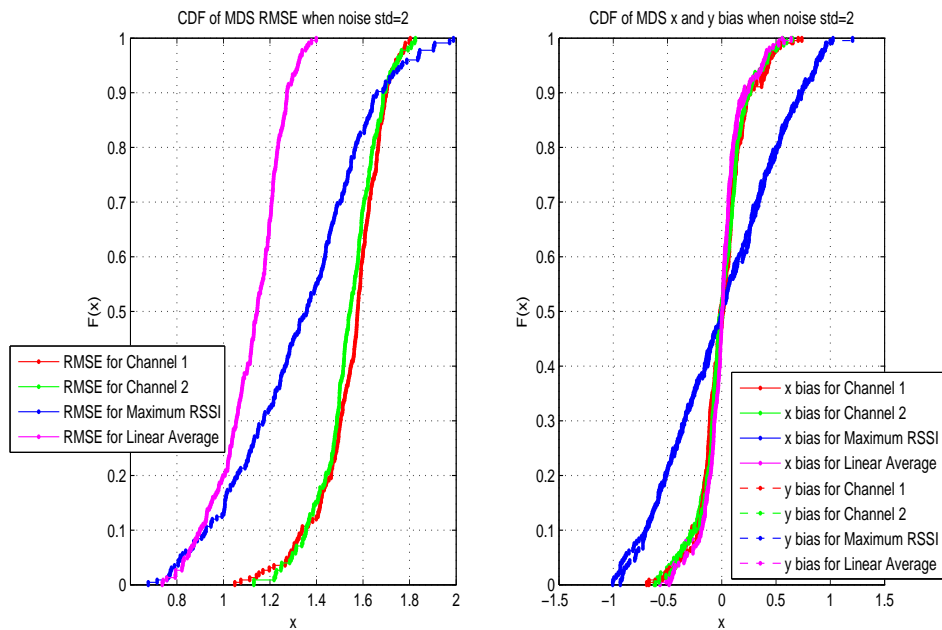


Figure A.5: CDF of MDS RMSE and Bias in 4 anchors with error std=2 case

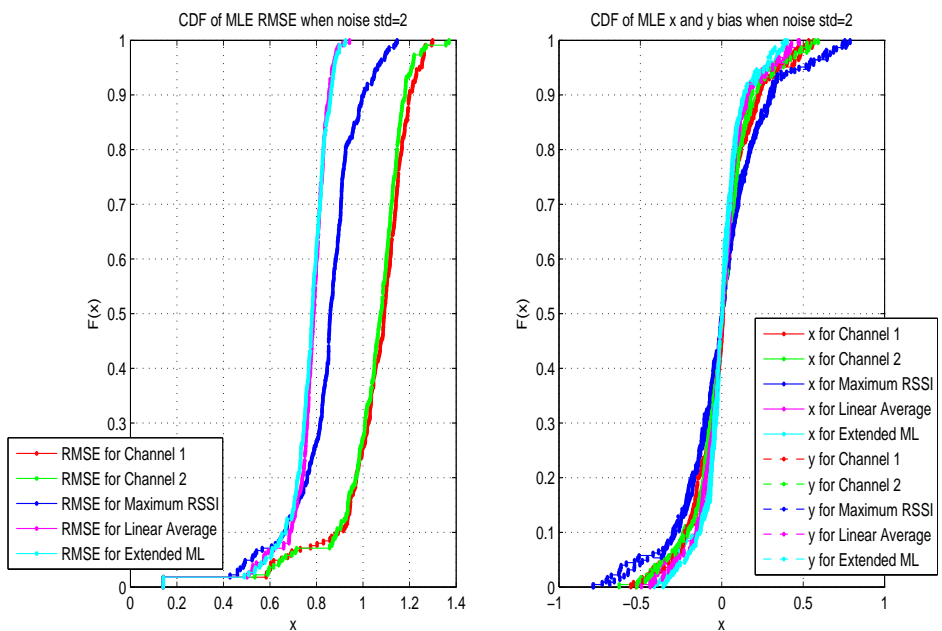


Figure A.6: CDF of MLE RMSE and Bias in 4 anchors with error std=2 case

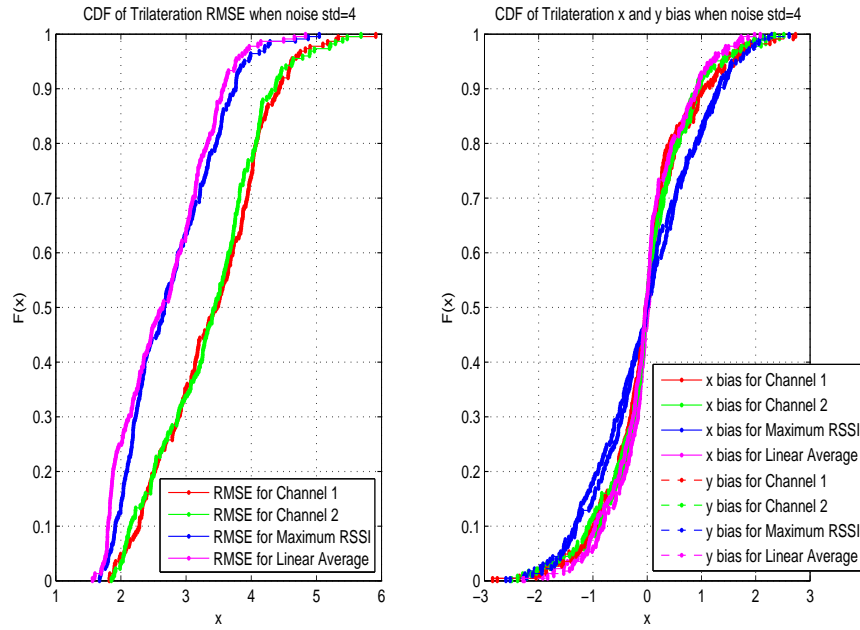


Figure A.7: CDF of Trilateration RMSE and Bias in 3 anchors with error std=4 case

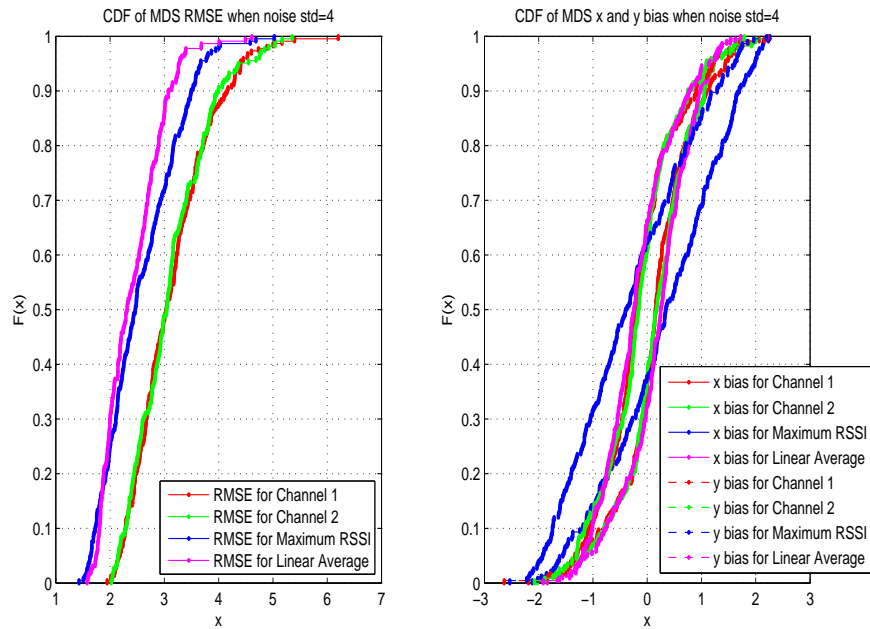


Figure A.8: CDF of MDS RMSE and Bias in 3 anchors with error std=4 case

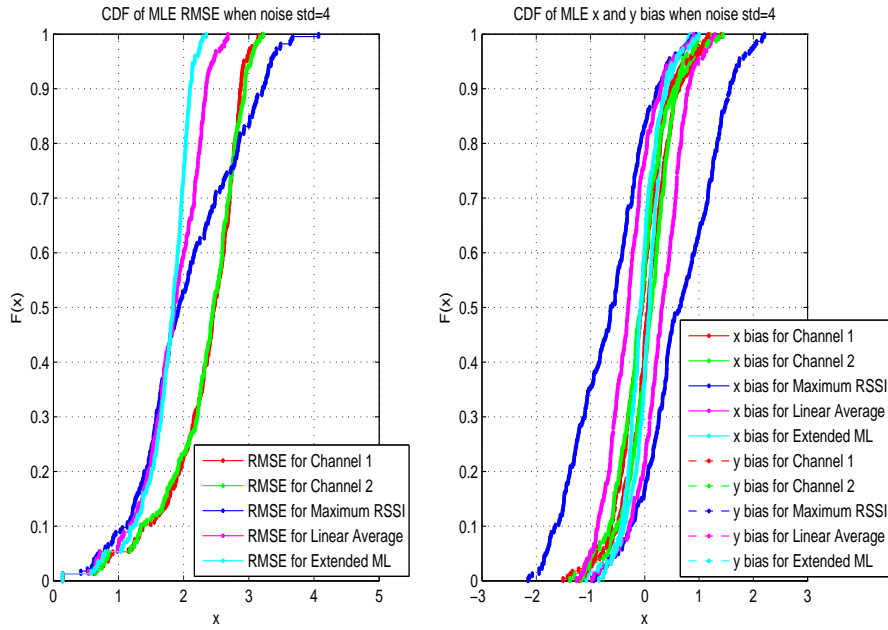


Figure A.9: CDF of MLE RMSE and Bias in 3 anchors with error std=4 case

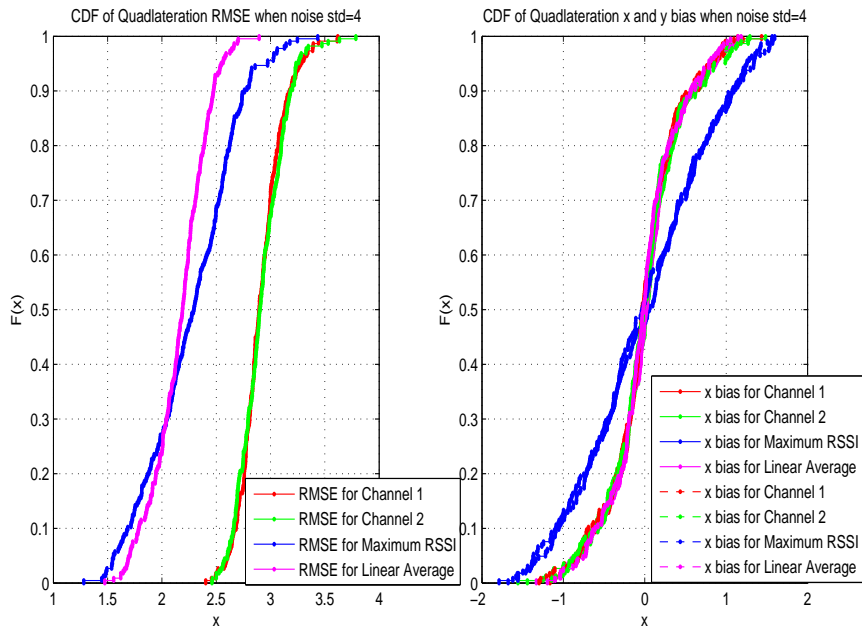


Figure A.10: CDF of Quadlateration RMSE and Bias in 4 anchors with error std=4 case

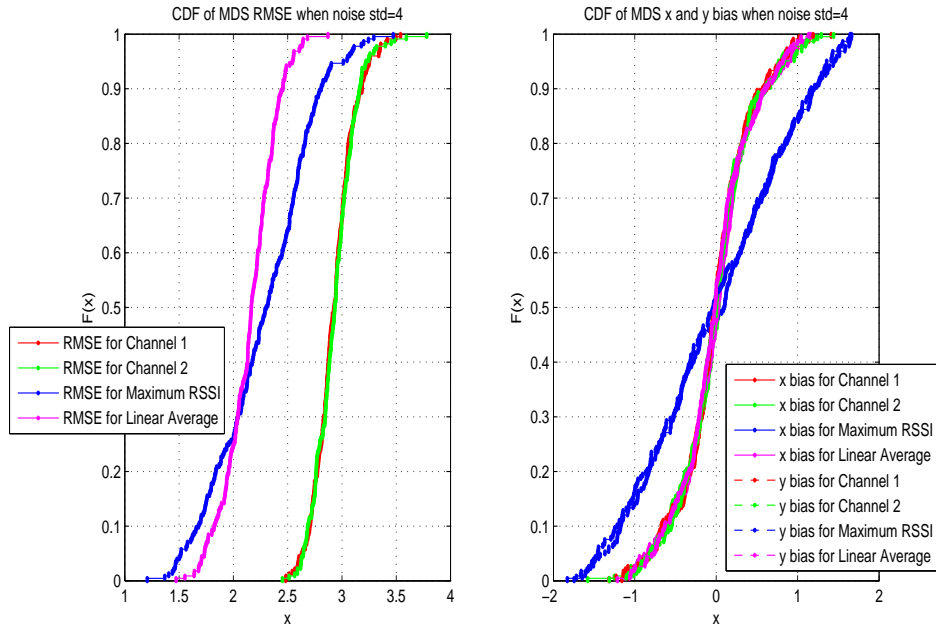


Figure A.11: CDF of MDS RMSE and Bias in 4 anchors with error std=4 case

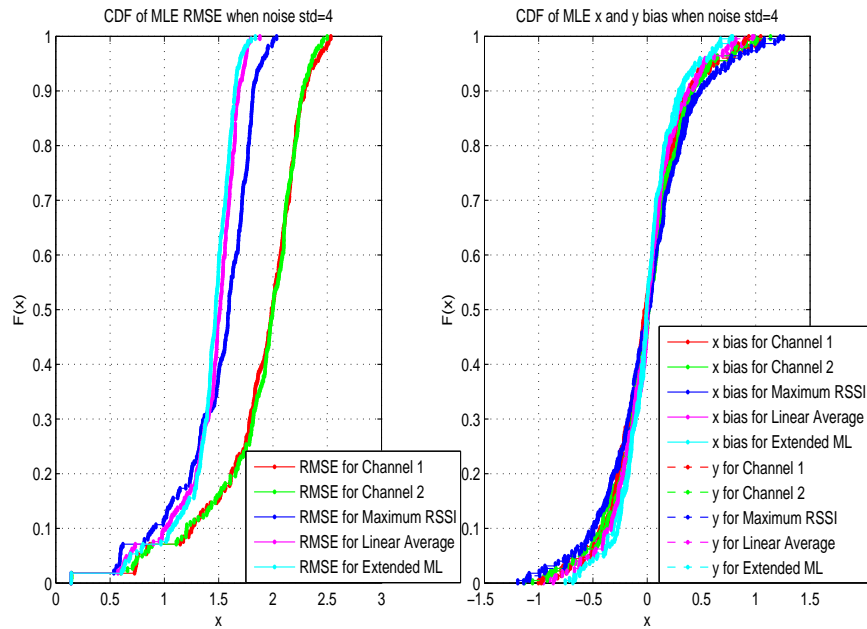


Figure A.12: CDF of MLE RMSE and Bias in 4 anchors with error std=4 case

REFERENCES

- [1] R. Akl, D. Tummala, and X. Li. Indoor propagation modeling at 2.4 GHz for IEEE 802.11 networks. In *Proceedings of the 6th IASTED International Multi-Conference on Wireless and Optical Communications*, July 2006.
- [2] I. Akyildiz, W. Su, Y. Sankarasubramaniam, and E. Cayirci. Wireless sensor networks: A survey. *Computer Networks (Elsevier) Journal*, 38(4):393–422, March 2002.
- [3] A. Bardella, N. Bui, A. Zanella, and M. Zorzi. An experimental study on 802.15.4 multichannel transmission to improve RSSI-based service performance. In *Proceedings of the 4th international conference on Real-world wireless sensor networks*, pages 154–161, 2010.
- [4] D. W. Bliss and K. W. Forsythe. Angle of arrival estimation in the presence of multiple access interference for CDMA cellular phone systems. In *Proceedings of the 2000 IEEE Sensor Array and Multichannel Signal Processing Workshop*, volume 1, pages 408–412, 2000.
- [5] M. Bor. Indoor localization for wireless sensor networks. Master’s thesis, Delft University of Technology, 2009.
- [6] I. Borg and P. Groenen. *Modern Multidimensional Scaling: Theory and applications*. Springer, 2005.
- [7] G. Calis, B. Becerik-Gerber, A. B. Goktepe, S. LI, and N. LI. Analysis of the variability of RSSI values for active RFID-based indoor applications. *Turkish Journal of Engineering and Environmental Sciences*, 37:186–210, July 2013.
- [8] G. Carter. *Coherence and Time Delay Estimation*. NJ:IEEE Press, 1993.
- [9] B. Champagne, S. Bedard, and A. Stephenne. Performance of time delay estimation in the presence of room reverberation. *IEEE Trans. on Speech and Audio Processing*, 4(2):148–152, March 1996.
- [10] F. Chan and H. So. Efficient weighted multidimensional scaling for wireless sensor network localization. *IEEE Trans. on Signal Processing*, 57(11):201–212, November 2009.
- [11] K. Cheng, K. Lui, and V. Tam. Localization in sensor networks with limited number of anchors and clustered placement. In *Proceedings of WCNC*, 2007.

- [12] T. Chrysikos, G. Georgopoulos, and S. A. Kotsopoulos. Impact of shadowing on wireless channel characterization for a public indoor commercial topology at 2.4 GHz. *ICUMT*, pages 281–286, 2010.
- [13] C. Diansheng, L. Xiyu, X. Wei, and W. Tianmiao. An improved quadrilateral localization algorithm for wireless sensor networks. *IEEE IICME International Conference on Complex Medical Engineering*, 2011.
- [14] Digi International. *XBee and XBee-PRO OEM RF Module Antenna Considerations*, June 2012.
- [15] Digi International. *XBee and XBee-PRO OEM RF Modules 802.15.4 Protocol*, March 2012.
- [16] S. Gezici. A survey on wireless position estimation. *Wireless Personal Communications*, 44(3):263–282, 2008.
- [17] G.Giorgetti, S.Kumar, S. Gupta, and G. Manes. Understanding the limits of RF based collaborative localization. *IEEE/ACM Trans. on Networking*, 19(6), December 2011.
- [18] A. Goldsmith. *Wireless Communications*. Cambridge University Press, 2005.
- [19] GP Batteries. *GP20R8HB*, 1st edition, 2009.
- [20] F. Gross. *Smart antennas for wireless communications*. NY: Mc Graw Hill, 2005.
- [21] Y. Gu, A. Lo, and I. Niemegeers. A survey of indoor positioning systems for wireless personal networks. *IEEE Communications Surveys and Tutorials*, 11(1), 2009.
- [22] J. Hightower and G. Borriello. Location systems for ubiquitous computing. *IEEE Computer Magazine*, 34(8):57–66, 2001.
- [23] K. Kaemarungsi. Design of indoor positioning systems based on location fingerprinting technique. Master’s thesis, University of Pittsburgh, 2005.
- [24] D. Koks. Numerical calculations for passive geolocation scenarios. *Technical Report DSTO-RR-0319*, 2007.
- [25] X. Li. RSS-based location estimation with unknown pathloss model. *IEEE Trans. on Wireless Communication*, 5(12):3626–3633, December 2006.
- [26] H. Lim and J. C. Hou. Localization for anisotropic sensor networks. In *Proceedings of IEEE InfoCom*, 2005.
- [27] B. Marcel, M. Clemens, A. Christian, S. Martin, and F. Florian. Analysis of radio signal parameters for calibrating RSSI localization systems. *Technical Report n455*, 2009.
- [28] National Research Council (U.S.). Committee on the Future of the Global Positioning System. *The Global Positioning System: A Shared National Asset*. National Academy Press, 1996.

- [29] D. Niculescu and B. Nath. Ad hoc positioning system (APS). In *Proceedings of GlobeCom*, volume 5, pages 2926–2931, November 2001.
- [30] D. Niculescu and B. Nath. Ad hoc positioning system (APS) using AoA. In *Proceedings of MobiCom*, 2003.
- [31] A. Pal. Localization algorithms in wireless sensor networks: Current approaches and future challenges. *Network Protocols and Algorithms*, 2(1):45–74, 2010.
- [32] N. Patwari. *Location Estimation in Sensor Networks*. PhD thesis, The University of Michigan, 2005.
- [33] N. Patwari, J. N. Ash, S. Kyperountas, A. O. Hero, R. L. Moses, and N. S. Correal. Locating the nodes: Cooperative localization in wireless sensor networks. *IEEE Signal Processing Magazine*, 22(4):54–69, July 2005.
- [34] N. Patwari, A. O. Hero, M. Perkins, N. S. Correal, and R. J. O’Dea. Relative location estimation in wireless sensor networks. *IEEE Trans. Signal Process.*, 51(8):2137–2148, Aug. 2003.
- [35] N. Patwari, R. J. O’Dea, and Y. Wang. Relative location in wireless networks. *IEEE VTC*, 2(8):1149–1153, May 2001.
- [36] N. B. Priyantha, A. Chakraborty, and H. Balakrishnan. The cricket location-support system. In *Proceedings of MobiCom*, pages 32–43, 2000.
- [37] T. Rappaport. *Wireless Communications*. Prentice Hall, 2002.
- [38] T. Rappaport, J. Reed, and B. Woerner. Position location using wireless communications on highways of the future. *IEEE Communications Magazine*, 34(10):33–41, 1996.
- [39] M. Rossi. RSSI-based tracking algorithms for wireless sensor networks: Theoretical aspects and performance evaluation. Master’s thesis, The University of Padova, 2007.
- [40] N. Salman, M. Ghogho, and A. Kemp. On the joint estimation of the RSS-Based location and path-loss exponent. *IEEE Wireless Communications Letters*, 1(1), February 2012.
- [41] A. Savvides, C. Han, and M. Srivastava. Dynamic fine-grained localization in ad-hoc networks of sensors. In *Proceedings of ACM MobiCom*, 2001.
- [42] A. Savvides, H. Park, and M. Srivastava. The bits and flops of the n-hop multilateration primitive for node localization problems. In *Proceedings of First ACM Int. Workshop WSN Appl.*, pages 112–121, September 2002.
- [43] A. Savvides, M. Srivastava, L. Girod, and D. Estrin. *Wireless sensor networks*. Kluwer Academic Publishers, 2004.
- [44] Y. Shang, W. Rumi, Y. Zhang, and M. Fromherz. Localization from mere connectivity. In *Proceedings of ACM MobiHoc*, pages 201–212, June 2003.

- [45] I. Stojmenovic. *Handbook of Sensor Networks: Algorithms and Architectures*. Wiley Interscience, 2005.
- [46] L. Tao, X. Shuai, C. Haiyong, and X. Hexu. Research on improved multidimensional scaling localization algorithm for wireless sensor network sensor network localization. In *Proceedings of International Conference on Optoelectronics and Image Processing*, November 2010.
- [47] H. Wymeersch, J. Lien, and M. Z. Win. Cooperative localization in wireless networks. In *Proceedings of IEEE*, volume 97, pages 427–450, February 2009.
- [48] S. Xi and M. D. Zoltowski. A practical complete MLE cooperative localization solution. In *Proceedings of ICASSP*, March 2010.
- [49] Y. Xiao, H. Chen, and F. Li. *Handbook on Sensor Networks*. World Scientific, 2010.
- [50] Z. Yang and Y. Liu. Quality of trilateration: Confidence-based iterative localization. *IEEE Trans. Parallel Distrib. Syst.*, 21(5):631–640, 2010.
- [51] H. Zepernick and T. Wysocki. Multipath channel parameters for the indoor radio at 2.4 GHz ISM band. In *Proceedings of IEEE Veh. Technol. Conference*, volume 1, pages 190–193, May 1999.
- [52] Y. Zhao, L. Dong, J. Wang, B. Hu, and Y. Fu. Collaborative localization with received signal strength in wireless sensor networks. *IEEE Trans. on Vehicular Technology*, 56(6):3807–3817, November 2007.
- [53] Y. Zhao, N. Patwari, P. Agrawal, and M. G. Rabbat. Directed by directionality: Benefiting from the gain pattern of active RFID badges. *IEEE Trans. on Mobile Computing*, 11(15), May 2012.